EVALUATION OF INTESTINAL MICROBIAL DIVERSITY AND A NEW ANTIBIOTIC REGIMEN IN CROHN'S DISEASE PATIENTS

by

KAREL P. ALCEDO
B.S. University of Central Florida, 2011

A thesis submitted in partial fulfillment of the requirements
for the degree of Master of Science
in the Burnett School of Biomedical Sciences
in the College of Medicine
at the University of Central Florida
Orlando, Florida

Fall Term
2015

Major Professor: Saleh A. Naser

ABSTRACT

Crohn's disease (CD) is a chronic granulomatous inflammatory bowel disease involving *Mycobacterium avium* subspecies *paratuberculosis* (MAP). Other microorganisms such as adherent-invasive *Escherichia coli* (AIEC) have also been proposed in CD association. To date, only one study investigated both MAP and AIEC simultaneously using peripheral blood but not in affected intestinal tissues. A standardized and effective antibiotic therapy against MAP and/or AIEC is needed for better treatment. Three antibiotic drugs – Clarithromycin (CLA), Rifabutin (RIF), and Clofazimine (CLO) have been used to treat CD patients suspected with MAP infection. However, the outcome has been controversial. The treatment dosage is high, the duration is long, and the reported drug side effects resulted in patient non-compliance; therefore, a lower and effective drug dosage is needed. In this study, we developed two aims 1) to evaluate RHB 104, a drug formula comprised of low dosages of CLA, RIF, and CLO, against clinical MAP strains *in-vitro* using fluorescence quenching method, and 2) to develop a fluorescence *in-situ* hybridization method to detect both MAP and AIEC simultaneously in intestinal tissues of CD patients. A total of 16 clinical MAP strains and 19 non-MAP strains were tested against varied concentrations of RHB 104, CLA, RIF, and CLO. Although the MIC for all drugs ranged between 0.5-20 μg/ml, the MIC for RHB 104 was significantly lower against most MAP strains. The effect of RHB 104 against MAP was bactericidal. Unlike RHB-104 formula, CLA, CLO, and RIF dosage similar to those in RHB-104 did not inhibit MAP growth when trialed individually and in dual-drug combinations. The data illustrated the presence of synergistic anti-MAP activity of low dosage of the three antibiotics in RHB-104.

We also developed a rapid and sensitive multicolor *in-situ* hybridization technique that can detect MAP and AIEC using tagged-oligonucleotide probes. Non-pathogenic *Escherichia coli*

(npEC) was used as a control for the study. Specifically, cultured MAP and npEC were fixed and hybridized with MAP488 and EC647 probes, respectively. Confocal laser scanning microscope (CLSM) revealed specific signals at 488nm for MAP and 647nm for npEC, indicating probe binding to each bacteria. This was confirmed with hybridization of MAP with EC647 and npEC with MAP488 resulting in absence of signals. Intestinal tissue samples from 9 CD patients were then analyzed using our technique. Preliminary data indicated positive results in 6/6 samples for MAP, 6/6 for npEC, 3/3 for AIEC, and 2/2 for both MAP and AIEC with MAP being more dominant. This protocol shortened the FISH procedure from multiple days to short-hours. The protocol allows the investigation of more than one pathogen simultaneously in the same clinical sample. A quantitative measurement of the signals is needed.

This is dedicated to Jerry & Nerie.

Ng dahil sa inyong dalawa, sa walang hanggang pagmamahal at paghihikayat niyo sa akin, sa pagsusuporta at pagdadasal, nakamit ko din ang aking mga pangarap.

ACKNOWLEDGMENTS

We would like to thank RedHill Biopharma, Ltd. for the financial support to the RHB 104 project and the Florida Legislative Grant for funding the second part of the study. We would also like to thank Dr. Seela Ramesh (Digestive and Liver Center of Florida) for his collaboration.

I am indebted to my advisor, Dr. Saleh Naser for providing me an opportunity to pursue research in his laboratory. I am very grateful for his guidance, support, and encouragement throughout the completion of my thesis. His passion for research and discovery has inspired me throughout and made this attainable. I would also like to thank my thesis committee members Dr. Zixi Cheng and Dr. Shadab Siddiqi for their guidance and assistance throughout this process. I would like to greatly appreciate Saisathya Thanigachalam for all her help, guidance, and friendship throughout these two years. I would like to thank Dr. Jeff Hatcher, Kristen Balkam, Dr. Alicja Copik, Jeremiah Oyer, Taylor Johnson, Robert Sharp, and all my fellow lab members for their assistance and encouragement.

I am grateful to my parents and siblings, my whole family and friends, who have unyielding support in me while I pursue my aspirations.

TABLE OF CONTENTS

LIST OF FIGURES x

LIST OF TABLES xii

LIST OF ABBREVIATIONS & ACRONYMS xiii

CHAPTER ONE: INTRODUCTION 1

CHAPTER TWO: IN-VITRO EVALUATION OF RHB 104 AGAINST CLINICAL STRAINS OF MYCOBACTERIUM AVIUM SUBSPECIES PARATUBERCULOSIS USING FLUORESCENCE QUENCHING-METHOD 3

Mycobacterium avium subspecies *paratuberculosis* 4

Treatment of Crohn's Disease 5

Antibiotic Drugs against Crohn's Disease 6

Materials and Methods 9

Mycobacterial Strains 9

IS900 Nested PCR 9

Antibiotic Drugs in Solution 10

Antibiotic Drug Susceptibility Test 10

RHB 104 Susceptibility Test 11

Determining the Synergistic Effects of the Antibiotic Drugs 11

RHB 104 Drug Stability Inhibitory Effect of RHB 104 11

Results 12

Confirmation of MAP identity using IS900 Nested PCR 12

Susceptibility of Mycobacterial strains against Clarithromycin, Clofazimine, Rifabutin, and RHB 104 12

Determining the Potency of RHB 104 13

Synergistic Effects in Combined Drug Therapy 14

Bactericidal or Bacteriostatic Effect of RHB 104 14

Discussion 14

CHAPTER THREE: DEVELOPMENT OF MULTICOLOR *IN-SITU* HYBRIDIZATION TECHNIQUE FOR DETECTION OF PATHOGENS FROM INTESTINAL MUCOSA OF CROHN'S DISEASE PATIENTS 28

Materials and Methods 31

Bacterial Strains 31

Tissue Samples 32

Preparation of oligonucleotide probes 32

Bacterial Fixation 33

Bacterial Fluorescent In-situ Hybridization 33

Fluorescent In-situ Hybridization on Intestinal Tissue Samples of CD Patients 34

Analysis 35

Results 35

Specificity of each oligonucleotide probe 35

FISHing for cultured MAP and npEC 35

FISHing for AIEC 36

FISHing for MAP, AIEC, and npEC on Intestinal Mucosa 36

Dual-FISH on tissue samples 37

Discussion 37

CHAPTER FOUR: CONCLUSION 48

REFERENCES 50

LIST OF FIGURES

Figure 1: Growth curve of *Mycobacterium avium* subspecies *Paratuberculosis*. 18

Figure 2: Representative agarose gel of MAP strains. 19

Figure 3: Representative agarose gel of IS900 nested-PCR products of MAP and non-MAP strains. 19

Figure 4: Potency of four antibiotic drugs against clinical MAP and non-MAP strains in vitro is shown using fluorescence quenching method. 20

Figure 5: Resistant non-MAP strains were inhibited at higher concentrations of four antibiotic drugs. 21

Figure 6: RHB 104 is potent at inhibiting MAP strain UCF 4 growth at low MIC levels. 22

Figure 7: RHB 104 inhibits *Mycobacterium avium*. 22

Figure 8: Clarithromycin, Clofazimine, and Rifabutin in RHB 104 showed synergistic effects against clinical MAP strains. 23

Figure 9: Two-drug combinations showed less potency of bacterial growth inhibition than RHB 104. 26

Figure 10: RHB 104 showed bactericidal activity against clinical MAP strain UCF 8. 27

Figure 11: BLAST analysis of the oligonucleotide probes for non-pathogenic EC, MAP, and AIEC. 41

Figure 12: FISHing for non-pathogenic *E. coli* using EC647. 42

Figure 13: FISHing for *Mycobacterium avium paratuberculosis* using MAP488 probe. 42

Figure 14: FISHing for non-pathogenic *E. coli* using the pathogenic probe AIEC546. 43

Figure 15: Non-pathogenic *E.coli* is present in the intestinal mucosa of Crohn's disease patients. 44

Figure 16: *Mycobacterium avium paratuberculosis* penetrated the lamina propria of intestinal tissues of CD patients..... 45

Figure 17: FISHing for adherent invasive *E. coli* in the intestinal tissues of CD patients. 46

Figure 18: Dual FISHing of intestinal tissues shows bacterial presence and co-localization. 47

LIST OF TABLES

Table 1: In-vitro activity of RHB 104, Clarithromycin, Clofazimine, and Rifabutin against clinical Mycobacterium strains 24

Table 2: In-vitro activity of 2-drug combinations in RHB 104 for their synergistic effects against MAP strain UCF 4 26

Table 3: Oligonucleotide Probes for MAP, pathogenic E. coli, and non-pathogenic E. coli 33

Table 4: Intestinal Tissue samples from Crohn's Disease patients. 40

LIST OF ABBREVIATIONS & ACRONYMS

5-ASA – 5-aminosalicylates

AIEC – Adherent-invasive *Escherichia coli*

BLAST – Basic local alignment search tool

CD – Crohn's Disease

CLA – Clarithromycin

CLO – Clofazimine

CLSM – Confocal laser scanning microscope

DAPI – 4',6-diamidino-2-phenylindole

diH_2O – Deionized water

DMSO – Dimethyl sulfoxide

DNA – Deoxyribonucleic acid

FDA – Food and Drug Administration

FISH – Fluorescent *in-situ* hybridization

GI – Gastrointestinal

HIV – Human immunodeficiency virus

IBD – Inflammatory bowel disease

IRB – Internal Review Board

JD – Johne's Disease

MAB – Monoclonal antibodies

MAC – *Mycobacterium avium* complex

MAP – *Mycobacterium avium* subspecies *paratuberculosis*

MGIT – *Mycobacteria* growth indicator tube

MIC – Minimum inhibitory concentration

NaCl – Sodium chloride (salt)

ND – Not determined

npEC – non-pathogenic *Escherichia coli*

PBS – Phosphate buffered saline

PCR – Polymerase chain reaction

RHB 104 – Cocktail antibiotic comprised of Clarithromycin, Rifabutin, and Clofazimine

RIF – Rifabutin

RNA – Ribonucleic acid

RT – Room temperature

SDS – Sodium dodecyl sulfate

SSC – Saline sodium citrate

TE – Tris-ethylenediaminetetraacetic acid

TNF-α – Tumor necrosis factor α

UCF – University of Central Florida

UV - Ultraviolet

CHAPTER ONE: INTRODUCTION

Crohn's Disease (CD) is a chronic inflammatory bowel disease with highly debated etiology that includes genetic predisposition and invasion of opportunistic pathogens. Patients with active CD generally present signs and symptoms similar to those observed in Johne's disease, an inflammatory bowel disease in cattle caused by *Mycobacterium avium* subspecies *paratuberculosis* (MAP)[1]. These include abdominal pain, diarrhea usually accompanied by the loss of blood, anemia, and weight loss[2, 3]. These clinical manifestations are commonly seen in other inflammatory bowel diseases in humans; therefore, in order to diagnose patients with CD, they must also present with intestinal granulomas observed during an ileocolonoscopy procedure[2]. Treatment for CD comprised immunosuppressive drugs to control the chronicity of inflammation in affected patients but they are not completely curative[4, 5]. Antibiotic regimen has also been used due to the isolation of opportunistic pathogens like MAP from the intestinal tissues, lymph nodes, blood, and breast milk of CD patients[4, 6-10]. A previous case study of a CD patient with MAP infection resulted in clinical healing and elimination of MAP infection after being administered an antibiotic regimen comprising of Clarithromycin and Rifabutin[11]. Because of this, a cocktail of antibiotics called RHB 104 was developed. RHB 104 comprises Clarithromycin, Rifabutin, and Clofazimine, and it is used against moderate to severely active CD in an on-going Phase III clinical trial. RHB 104 is comprised of lower dosages for each individual antibiotic drug than previously administered. The first part of this thesis is to evaluate RHB 104 against MAP *in-vitro* to determine its efficacy against this pathogen. Additionally, the synergistic effects of each drug at lower dosages in RHB 104 will be evaluated *in-vitro* against clinical MAP strains.

Although MAP has been associated with CD for a century, another leading pathogen under investigation for possible etiological agent is adherent-invasive *Escherichia coli*. AIEC has also been isolated from intestinal tissues, lymph nodes, and blood of CD patients[12-14]. Both MAP and AIEC have been studied simultaneously from the peripheral blood of CD and non-CD patients[10]; however, they have not been studied together simultaneously from intestinal tissues. The second part of this thesis is to develop a fluorescence *in-situ* hybridization method to detect these two opportunistic pathogens from the intestinal tissues of patients with Crohn's disease. This enables visualization of these pathogens *in-situ*, circumventing the need for isolation and culture of MAP and AIEC. It also determines the spatial distribution of each pathogen within and around affected tissues. This technique enables quantification of the prevalence of MAP and AIEC in intestinal tissues of CD patients. Lastly, it enables delineation of the potential role of MAP or AIEC as the causative agent or opportunistic agents that exacerbate inflammation in CD.

CHAPTER TWO: IN-VITRO EVALUATION OF RHB 104 AGAINST CLINICAL STRAINS OF MYCOBACTERIUM AVIUM SUBSPECIES PARATUBERCULOSIS USING FLUORESCENCE QUENCHING-METHOD

Crohn's disease (CD) is a chronic inflammatory bowel disease of debated etiology. Possible causes include genetic predisposition, immune dysregulation, and environmental factors. CD affects about 10.7 per 100,000 people-years in North America[15], and 6.3 per 100,000 people-years in Europe[16]. Despite the low incidence of CD in Asia[17] and Africa, recent epidemiological studies have shown an increasing number of affected individuals in these continents[18-20]. Patients diagnosed with CD suffer from excessive and/or nocturnal diarrhea, abdominal pain, and rapid weight loss, all of which affect their quality of life[21]. Histologically, a cobblestoned appearance of the mucosal layer and granulomas scattered in the intestines, particularly in the distal ileum and colon, are observed in CD patients[22]. Similarly, these clinical and pathological manifestations have been observed in Johne's disease (JD), a chronic granulomatous inflammation of the intestines in ruminants. JD is caused by an intracellular pathogen called *Mycobacterium avium* subspecies *paratuberculosis* (MAP)[1]. Because of this and mounting evidence of the presence and isolation of MAP from humans, MAP has been indicated as an etiological agent of CD[7, 8]. Open and randomized clinical trials of anti-MAP therapy comprising of Clarithromycin (CLA), Clofazimine (CLO), and Rifabutin (RIF) have shown auspicious results[11, 23, 24]. However, the drug dosages are high and the course of therapy is long. These can pose problems such as dysbiosis of normal gut flora and/or exacerbation of prevailing gastrointestinal (GI) symptoms such as diarrhea and stomach pain; thus, a low, effective drug dosage is always sought after. RHB 104 is a drug formula that is composed of all three antibiotic drugs at lower dosages than those used in previous studies. It has been recently approved by the United States Food and Drug Administration (FDA)

to treat patients with moderate to severe CD in an on-going Phase III clinical trial. This study is designed to evaluate RHB 104 *in-vitro* against clinical MAP strains from CD patients. Our data suggests that the combination of lower dosages of each drug in RHB 104 has a higher efficacy of anti-MAP activity.

Mycobacterium avium subspecies *paratuberculosis*

MAP is a ubiquitous, obligate pathogen that thrives in its environment such as soil, pasteurized milk, meat products, and drinking water[25-30]. MAP is also resistant to chlorination and pasteurization; therefore, it is not easily eliminated[31]. Since 1913, it has been suggested by Dr. Dalziel that MAP may play a role in the pathogenesis of CD, and was further examined after its isolation from humans by Chiodini, et al[7]. MAP is a spheroplast in humans, meaning it is cell wall deficient[8]; as such, it cannot be identified easily by Ziehl-Neelsen acid fast staining. Furthermore, MAP does not produce mycobactin, an iron-chelator that is essential to its growth and replication[32]. As a result of both of these characteristics, culturing MAP from humans is extremely difficult. However, with the improvement in culturing techniques, MAP isolates from human samples can show positive growth in culture medium. Additionally, MAP is considered to be one of the slowest growing mycobacteria in culture, taking between 3 to 6 months, further prolonging detection[33]. An alternative way to detect the presence of MAP from human samples is by using *IS900* nested polymerase chain reaction (Nested PCR), which amplifies 298 base pairs of the insertion sequence gene that has 15-18 copies in MAP DNA only[34]. Using the improved culturing technique and Nested PCR, MAP has been isolated and identified from peripheral blood, intestinal tissues, CD lesions, lymph nodes, and breast milk of CD patients[8, 9, 34, 35]. Regardless of this evidence, a possible relationship between MAP and CD remains controversial because MAP is

also present in healthy or non-CD individuals[10, 36, 37]. An effective anti-MAP therapy for CD such as the combination in RHB 104 may provide further support to the MAP hypothesis by complete elimination of MAP concurrent to healing in CD patients.

Treatment of Crohn's Disease

Current treatment mainly focuses on alleviating the symptoms experienced by CD patients. The most prominent being chronic inflammation in different parts of the GI tract that may lead to complications such as stricture formation, ulceration, and fistulization[38-42]. CD requires medical and surgical treatment; however, medical treatment is considered the first choice in treating and managing it. Medical treatment encompasses the use of anti-inflammatory drugs, immunosuppresants, nutritional therapy, and antibiotics[38, 43-45]. If severe complications develop, surgical treatment becomes necessary, which includes laparoscopy, strictureplasty, anastomosis, resection, or bypass surgery[38, 39]. These surgical methods are costly and time-consuming, and they alter patients' lifestyles, especially when there is a recurrence of CD.

Chronic inflammation as a result of CD can be managed using anti-inflammatory drugs such as 5-aminosalicylates (5-ASA) and steroids, or monoclonal antibodies (MAB) such as Infliximab (Remicade) and Adalumimab (Humira)[46]. 5-ASA works in multiple ways, such as suppressing the production of platelet activating factor[47], which is a pro-inflammatory mediator, and decreasing the expression of interferon-γ[48, 49]. Steroids work similarly to 5-ASA by downregulating the production of pro-inflammatory mediators and cytokines. Current MAB therapy, on the other hand, targets and blocks TNF-α from mediating an inflammatory response and recruiting immune cells to the site of infection. Both anti-inflammatory drugs and MAB therapy have been reported to manage the symptoms experienced by CD patients, but relapse

occurs after cessation of treatment[50-52]. These treatments are costly with insufferable adverse effects that include but are not limited to dependency on steroids, hypersensitivity, hepatic injury, and potential excessive immune suppression leading to re-infection[53, 54]. A more effective therapy for CD should induce and maintain remission without any relapse, with the additional benefits of lessening the gastrointestinal adverse effects.

Antibiotic Drugs against Crohn's Disease

Recently, the emergence of multiple studies on the presence of pathogens in the gut of CD patients, most notably of the presence of MAP, have led to the usage of antibiotic treatments. MAP is closely related to the family of *Mycobacterium avium* complex (MAC), a pathogen infecting HIV or immunosuppressed patients. Anti-tuberculosis drugs have not been effective against MAC; however, other antibiotics such as Clarithromycin and Rifabutin have shown efficacy. Clarithromycin is a macrolide antibiotic that targets the 50S ribosomal subunit and inhibits protein synthesis[55]. Monotherapy with Clarithromycin showed effective inhibition of MAC; however, this regimen is futile because of the possible development of antibiotic resistance[56, 57]. Another drug or combinatory antibiotic therapy was sought after. Rifabutin, a derivative of Rifamycin, has also been shown to effectively inhibit MAC growth[58, 59]. Rifabutin is an antibiotic drug that targets the mycobacterial RNA polymerase, thus preventing transcription elongation[58, 60, 61]. This mechanism of action leads to its bactericidal property. Both Clarithromycin and Rifabutin have been used in a combinatory regimen against MAC in HIV-AIDS patients and have shown to be effective with lesser adverse effects[62].

The therapeutic regimen seen in MAC infection with the combinatory anti-mycobacterial drugs was adopted because of the similarity of MAC and MAP. More importantly, these antibiotic

drugs can also target the cellular machinery within MAP instead of targeting its cell wall, which is lacking in MAP found in humans. Several randomized clinical trials using anti-MAP regimen in CD patients have shown promising results[4, 63]. Gui et al in their 1997 study reported the use of RIF and CLA[64]. In 93.5% of CD patients using the regimen (RIF-CLA), clinical remission indicated by improvement in the Harvey-Bradshaw activity index was achieved. Initial steroid use was also discontinued during the study. Another clinical trial using the same treatment showed clinical improvement in 58.3% of CD patients, with complete healing of ulcers seen after >6 months of treatment[24]. A 2007 case study reported that a patient, who was suffering from recurrence of severe CD and was being treated with anti-inflammatory drugs, attained complete clinical remission using anti-MAP therapy[11]. These studies showed the profound effects of anti-MAP therapy in CD.

Moreover, Borody et al has added Clofazimine to the anti-MAP therapy since it also targets the transcription of DNA similar to Rifabutin[63]. Clofazimine, an antibiotic drug that is most commonly used against leprosy, also exerts activity against mycobacteria by interacting with an oxidoreductase in the respiratory chain to produce reactive oxygen species[65, 66]. The anti-MAP therapy then comprised of Clarithromycin, (500-750 mg/day), Rifabutin (450 mg/day) and Clofazimine (100 mg/day)[23]. Clinical trials have reported efficacy of this triple anti-mycobacterial drug combination and >50% patients achieved prolonged clinical remission. Longitudinal scarring receded to normal mucosa that further led to mucosal healing from multiple ulcerations in patients with moderate to active CD after taking the drug combination[23, 63]. In 2007, the largest clinical trial to date also used the triple anti-MAP therapy[4]. Selby et al reported clinical remission in 66% of patients after 16 weeks of treatment. During the maintenance phase of the study, patients under the antibiotic treatment showed less relapse than those of the control, providing more evidence of

the effects of the anti-MAP regimen. Despite these reported prolonged remission and mucosal healing, there were patients unaffected by the therapy or who experienced recurrence of CD during therapy. Some patients in these clinical trials were also excluded because of adverse effects from the drugs. These adverse effects include: general malaise, fatigue, headache, arthralgia, abnormal liver enzyme levels, leukopenia, and jaundice. In addition, abdominal pain, nausea, vomiting and diarrhea, which are common side effects from all three drugs, were also observed from the participants of the studies. One possible cause of this is the high dosage administered to patients for each individual antibiotic drug for a long duration of treatment lasting 12 months to more than 2 years, thus, exacerbating the GI symptoms experienced in CD. Furthermore, the long duration of treatment of a cocktail of antibiotics taken daily can be costly and can prevent the patients from being compliant in medicating. A single drug like RHB 104 that combines low and effective dosages of individual anti-MAP drugs is needed.

RHB 104 is a combinatorial antibiotic drug composed of 95 mg Clarithromycin (63.3%), 10 mg Clofazimine (6.7%), and 45 mg Rifabutin (30%). Each drug concentration is lower in RHB 104 than initially used in previous clinical trials. It is undergoing Phase III clinical trials for moderately to severely active CD in several countries. Our study is aimed to parallel the on-going clinical trial by investigating the activity of RHB 104 in eliminating clinical MAP strains *in-vitro*. In order to do this, we evaluated the activity of RHB 104 and each individual drug or two-drug combinations at their levels in RHB 104 against clinical MAP strains.

Materials and Methods

Mycobacterial Strains

A total of 35 *Mycobacterium* species were used for the drug susceptibility project (Table 1). It includes 16 clinical MAP strains, 10 *Mycobacterium avium* strains and 9 other *Mycobacterium* species. All 16 MAP samples were obtained from the -80˚C freezer, thawed out, and cultured in BD Bactec™ MGIT™ Para-TB medium (Sparks, MD) with growth supplement and mycobactin J. Other *Mycobacterium* species such as *M. tuberculosis, M. smegmatis, M. intracellulari* and others were also obtained from -80˚C freezer, thawed out, and cultured in BD Bactec™ MGIT™ TB medium (Sparks, MD) with growth supplement. They were incubated at 37˚C. Growth was measured initially using the UV illuminator (Andromeda). The medium contains a fluorescent molecule embedded in silicone that is oxygen sensitive, and will fluoresce in the presence of active respiring mycobacteria. Fluorescence quenching or the absence of fluorescence is indicative of no growth. Latter experiments were incubated at 37˚C in BD Bactec™ MGIT™ 320 instrument, which measures the intensity of fluorescence, emitted and converts the value to a measurable growth unit. A growth unit of 75 or higher is indicative of positive growth (Figure 1).

IS900 Nested PCR

All 35 mycobacterial samples were subjected to *IS900* nested PCR to confirm their MAP identity. DNA extraction was followed per protocol as published by our group[9]. The first of two rounds of PCR used P90/P91 primers (5'-GTTCGGGGCCGTCGCTTAGG-3'/5'-GAGGTCGATCGCCCACGTGA-3') to amplify 398 bp of the *IS900* gene in MAP DNA. Subsequently, the products of the first round of PCR were used as samples for the second round.

The secondary primers were AV1/AV2 (5'-ATGTGGTTGCTGTGTTGGATGG-3'/5'-CCGCCGCAATCAACTCCAG-3'), amplifying 298 bp from the initial products. Amplified PCR products were separated using agarose gel electrophoresis, and the bands were visualized using ethidium bromide under the UV illuminator (Andromeda).

Antibiotic Drugs in Solution

Clarithromycin (CLA), Clofazimine (CLO), and Rifabutin (RIF) were kindly provided by the manufacturer. The stock solution for Clarithromycin (1 mg/ml) was prepared using sodium acetate in water (pH 5.0). The stock solution for Clofazimine (1 mg/ml) was prepared using hydrochloric acid and sodium dodecyl sulfate in water. The stock solution for Rifabutin (1 mg/ml) was prepared using absolute methanol[67].

RHB 104 was also kindly provided by the manufacturer. Due to the unavailability of the patent-protected solvent to dissolve RHB 104, we reconstructed it by dissolving each individual drug (CLA, CLO, RIF) in their respective solvents. Clarithromycin, Clofazimine, and Rifabutin were combined per their percent composition (63.3% Clarithromycin, 30% Rifabutin, and 6.7% Clofazimine) in RHB 104.

Antibiotic Drug Susceptibility Test

The minimum inhibitory concentration (MIC) was determined for each of the three antibiotic drugs. In a BD Bactec™ MGIT™ Para-TB medium, 200 μL of mycobacterial sample (10^5 to 10^6 colony-forming units/ml) and 800 μL of growth supplement were added. Mycobactin J was added in MAP samples. Subsequently, each antibiotic drug was added in to each respective

culture medium at concentrations ranging between 0.5 μg/ml – 20 μg/ml. Controls were established in culture medium without any antibiotic drugs. All samples were incubated at 37˚C.

RHB 104 Susceptibility Test

The MIC of RHB 104 was also determined by inoculating mycobacterial samples with RHB 104 per above protocol. The concentrations tested ranged between 0.5 μg/ml – 20 μg/ml of RHB 104 against all mycobacterial samples. Controls were also established in culture medium without RHB 104. All samples were incubated at 37˚C.

Determining the Synergistic Effects of the Antibiotic Drugs

To determine the synergistic effects of the three antibiotic drugs in RHB 104, 2-drug combinations of CLA-CLO, CLA-RIF, and CLO-RIF were established (Table 2) and used against mycobacterial samples grown in BD Bactec™ MGIT™ TB Medium. Growth supplement for all samples and mycobactin J for all MAP samples were added. These were incubated at 37˚C in BD Bactec™ MGIT™ 320 instrument.

RHB 104 Drug Stability Inhibitory Effect of RHB 104

Samples from the MIC/drug susceptibility experiments showing negative growth without fluorescence under the UV illuminator as well as those reported with zero growth units were used. Positive controls were taken from the same samples incubated without RHB 104. They were washed twice with TE buffer at 13,200 rpm for 2 minutes. The pellets were re-suspended in 800 μL of growth supplement. Each sample was added in to each respective fresh BD Bactec™ MGIT™ TB medium with 8 μL mycobactin J and incubated at 37˚C.

Results

Confirmation of MAP identity using IS900 Nested PCR

IS900 nested PCR was used on all 35 mycobacterial samples to identify MAP DNA and confirm their identity. An agarose gel in Figure 2&3 showed bands at 398 bp for the primary PCR, and lower bands at 298 bp for the secondary PCR for all MAP strains, and absence of bands for all non-MAP strains. There was a total of 16/35 MAP strains, 10/35 *M. avium* strains, and 10 other *Mycobacterium* species.

Susceptibility of Mycobacterial strains against Clarithromycin, Clofazimine, Rifabutin, and RHB 104

The MIC for Clarithromycin, Clofazimine, Rifabutin, and RHB 104 against all 35 mycobacteria strains are given in Table 1. Initially, we utilized the fluorescence quenching method to determine the *in-vitro* activity of RHB 104 and its individual antibiotic components (CLA, CLO, and RIF) against all strains (representative samples are shown in Figure 4). The absence of fluorescence in each culture medium indicated growth inhibition of mycobacteria. MIC was read and reported as the concentration from the first culture medium showing absence of fluorescence. In 81% (14/16) MAP strains that were tested, the MIC for all drugs was reported to be $\leq$ 1 μg/ml. In 13% (2/16) MAP strains, the reported MIC for CLA, RIF, and RHB 104 were $\leq$ 4-6 μg/ml, but the MIC for CLO is higher at >6 μg/ml. An exception was MAP strain UCF 10, which had an MIC of >10 μg/ml in all drugs but CLA at <10 μg/ml. Among non-MAP strains, the MIC for all drugs was higher (representative samples shown in Figure 5). In 70% (7/10) of *M. avium* strains, the reported MIC for CLA, RIF, and CLO were >6 μg/ml, whereas the MIC for RHB 104 was $\geq$ 4 μg/ml. *M. avium* strain JF1 had MIC for all drugs at >10-20 μg/ml. *M. avium* strain NEZ was only

tested at 1 μg/ml for all drugs and it showed resistance at this level. *M. avium* was inhibited at <4 μg/ml of CLA and RHB 104, whereas for CLO and RIF, the MIC was at >6 μg/ml. Other non-MAP strains were more resistant with reported MIC for all drugs in the range of 6-20 μg/ml.

The data for RHB 104 was confirmed by growth unit readings using BD Bactec™ MGIT™ 320 instrument. RHB 104 was tested against MAP UCF 4 and complete growth inhibition was achieved at an MIC of 0.4 μg/ml (Figure 6). In contrast, the MIC for RHB 104 against *M. avium* was 3 μg/ml (Figure 7). Both values correspond to what was qualitatively shown by fluorescence quenching method (Figure 4). Overall, Clarithromycin, Clofazimine, Rifabutin, and RHB 104 had a more potent effect at lower dosages against clinical MAP strains compared to other non-MAP strains.

Determining the Potency of RHB 104

Although Table 1 showed similar MIC for all four drugs, the potency of RHB 104 was determined by comparative analysis. RHB 104 at a concentration of 1 μg/ml contains 633 ng/ml of CLA, 300 ng/ml of RIF, and 67 ng/ml of CLO. The concentrations of each individual drug at the levels of the MIC for RHB 104 against each sample were calculated (Table 1). In all samples tested, 54% (19/35) showed resistance to CLA, RIF, and CLO at their levels in the MIC for RHB 104 for each bacteria. In clinical MAP strains, 19% (3/16) showed susceptibility to CLA but resistance to CLO and RIF at the levels in 1 μg/ml of RHB 104 (Figure 8). The remaining non-MAP samples showed resistance to CLA, RIF, and CLO at their individual levels in RHB 104 (Table 1).

Synergistic Effects in Combined Drug Therapy

In order to further analyze the synergistic effect of CLA, RIF, and CLO in RHB 104, we tested the activities of 2-drug combinations against MAP UCF 4 as shown in Figure 9. The drug combination of CLA-CLO and CLA-RIF had 100% inhibition against clinical MAP strains at their levels in 0.5 μg/ml RHB 104. The combination of CLO-RIF only reached 86% inhibitory effect against clinical MAP strains at their levels in 1 μg/ml RHB 104. A comparison between the MIC of each drug individually and in combination with one other drug is shown in Table 2. The MIC of each individual drug against clinical MAP strains is higher than when combined with each other.

Bactericidal or Bacteriostatic Effect of RHB 104

The inhibitory effect of RHB 104 was demonstrated using fluorescence quenching method as shown in Figure 10. A volume of MAP strain UCF 8 sample taken from culture with 1 μg/ml of RHB 104 showed no growth by means of the absence of fluorescence after re-inoculation in to fresh medium within 32 days. The positive control showed active growth at day 4 post-inoculation. To confirm the bactericidal effect of RHB 104, a repeat of this experiment using MAP strain UCF 4 from culture with 1 μg/ml RHB 104 was re-inoculated in to fresh medium, and incubated in the Bactec™ MGIT™ 320 instrument. The result for this experiment is pending growth unit readings.

Discussion

Anti-MAP regimen, which includes Clarithromycin, Rifabutin, and Clofazimine, has been investigated in multiple clinical trials as possible treatment for Crohn's disease due to *Mycobacterium avium* subspecies *paratuberculosis* being implicated as its etiological agent[4, 23, 24, 63]. RHB 104 is a new combinatorial drug comprised of the anti-MAP regimen at lowered dosages

than previously administered to patients. In this study, we aimed to evaluate the efficacy of RHB 104 against clinical MAP strains.

Initially, we evaluated each individual drug in RHB 104 to determine their potency against 16 clinical MAP strains and 19 non-MAP strains. Our data for the MIC of each individual drug were comparable to previous studies that reported the MIC for Clarithromycin in the range of 0.25-0.5 μg/ml, Clofazimine at 0.5-1 μg/ml, and Rifabutin at 0.3-0.5 μg/ml[68-70] against clinical MAP strains[71]. Representative samples of non-MAP strains such as *M. Smegmatis, M. intracellulari* and *M. avium* were susceptible at higher dosages of >4-20 μg/ml of CLA, CLO, and RIF. We also evaluated the efficacy of RHB 104 against all 35 mycobacterial samples. Unfortunately, we were not able to dissolve RHB 104 in any diluent including those used for CLA, CLO, and RIF. In order to replicate RHB 104, we combined each of the three drugs per their percent composition. We obtained the MIC for RHB 104 in the range of 0.25-1 μg/ml against clinical MAP strains. Conversely, the MIC for all drugs against non-MAP strains such as *M. avium, M. smegmatis,* and *M. intracellulari* were in the range of 4-20 μg/ml, showing more resistance to RHB 104 than clinical MAP strains. Overall, our data have shown that all three drugs and RHB 104 are more efficacious against clinical MAP strains in contrast to non-MAP strains, reporting their MICs to be lower.

Although the MIC for RHB 104 seems comparable to the MIC for each of the 3 individual drugs, it has to be noted that the dosages for each drug is lower in RHB 104. In that case, a reported MIC of 1 μg/ml for RHB 104 actually contains 0.633 μg/ml of CLA, 0.30 μg/ml of RIF, and 0.067 μg/ml of CLO. While Clarithromycin appears to be potent in bacterial inhibition at less than 633 ng/ml or 0.63 μg/ml, it is futile to treat patients with one antibiotic drug for more than a year

because of possible development of antibiotic resistance. A combination of antibiotic drugs such as in RHB 104 can eliminate the problem with resistance while exhibiting anti-MAP activity. In this study, we evaluated CLO and RIF individually at their levels in 1 μg/ml of RHB 104 against clinical MAP strains. Our reports showed that both drugs at lower concentrations are not effective at bacterial inhibition by themselves. This showed that there may be some synergistic effect between low dosages of CLA, CLO, and RIF when combined in RHB 104. We created dual combinations of CLA-CLO, CLA-RIF, and CLO-RIF and tested them against clinical MAP strains and other non-MAP strains. Our data showed that the dual combination of CLA-CLO and CLA-RIF was the most effective at completely inhibiting mycobacterial growth at their levels in 0.5 μg/ml of RHB 104, particularly against clinical MAP strains. The combination of RIF and CLO was the least effective at bacterial inhibition, even at their levels in 1 μg/ml RHB 104, but still exhibited some anti-MAP activity. This was expected as this combination contains 2 drugs with lower concentrations in RHB 104. The combinations with CLA showed the highest anti-MAP activity. Although CLA may be the biggest player within these combinations, again, monotherapy with Clarithromycin may lead to antibiotic resistance. In contrast to the 2-drug combination, RHB 104 showed effective inhibition at a lower concentration of 0.25 μg/ml against clinical MAP strain. This showed that the 3 drugs are synergistic and effective at lower concentrations against MAP than when used individually or in 2-drug combinations. It showed the superiority of RHB 104 and its anti-MAP activity in contrast to the 3 drugs individually or in dual combination with each other.

Our data also showed the bactericidal activity of RHB 104 against clinical MAP strains. This was exhibited when MAP harvested from a culture with RHB 104 did not grow in fresh MGIT medium with no drugs. This can be attributed to the mechanism of action of all three drugs CLA, CLO, and RIF that target the transcription and translation machinery within the bacteria. MAP in

humans lack its cell wall; therefore, using antibiotic drugs that target the cell wall will not only be inefficient for treatment of CD, but it may also lead to complications by inhibiting some normal flora. The combination of drugs in RHB 104 was wisely chosen as anti-MAP regimen from a wide range of antibiotic drugs.

Our findings showed effective *in-vitro* activity of RHB 104 against clinical MAP strains, as well as non-MAP strains. In parallel, if RHB 104 induces and maintains clinical remission in CD patients from the Phase III clinical trial of RHB 104, then this will provide more evidence in the MAP theory as a causative agent in CD.

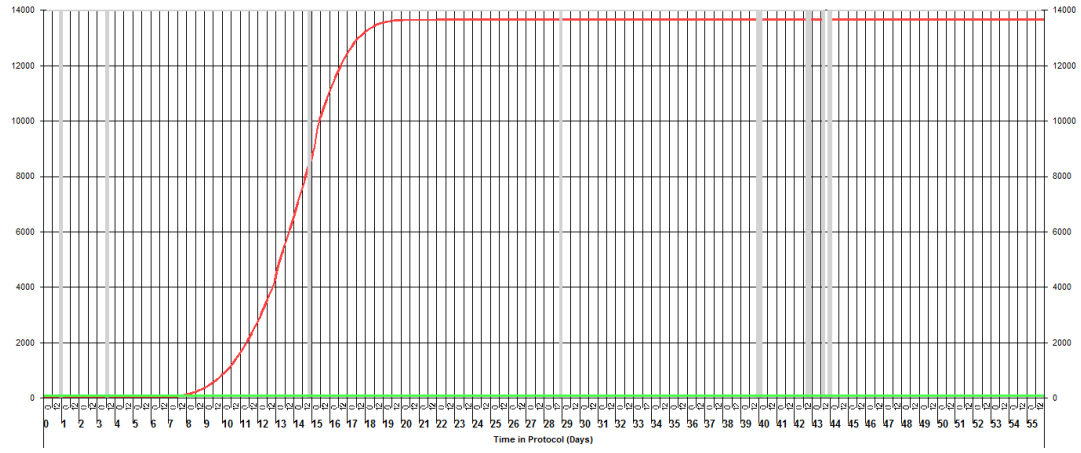

Figure 1: Growth curve of *Mycobacterium avium* subspecies *Paratuberculosis*. MAP strain UCF 4 was inoculated in a MGIT medium with OADC growth supplement and mycobactin J. It was incubated at 37°C in BD Bactec™ MGIT™ 320 instrument. Growth was detected after 7 days of inoculation.

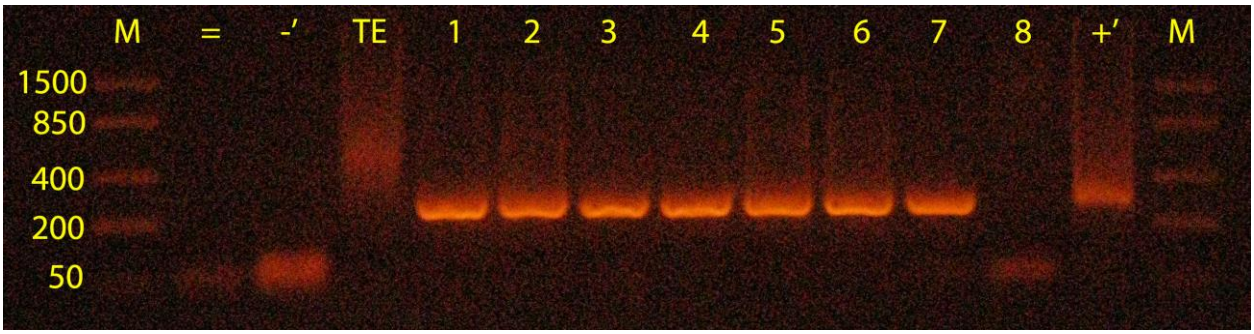

Figure 2: Representative agarose gel of MAP strains. *IS900* nested polymerase chain reaction (*IS900* Nested-PCR) goes through two rounds of PCR to confirm the identity of clinical MAP strains **1)** UCF 5 **2)** UCF 8 **3)** MAP 7 **4)** MAP 8B **5)** MAP Ben **6)** MAP Kay **7)** MAP Linda **8)** MAP Para 18. The 298 bp amplicon from each clinical MAP strain is identical to the positive control.

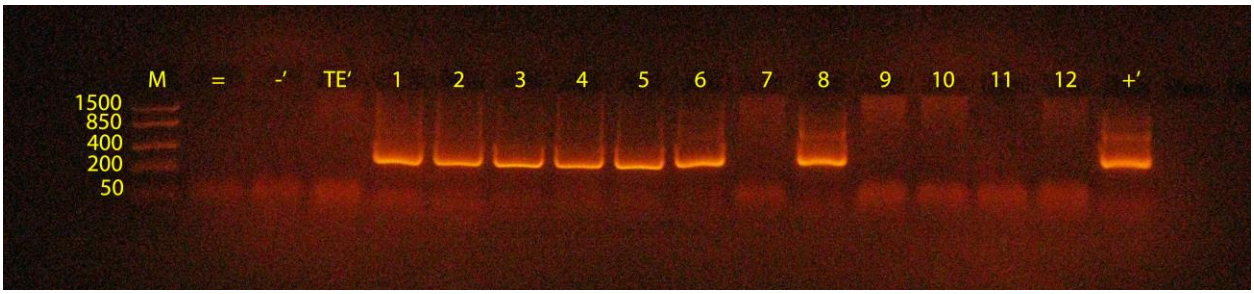

Figure 3: Representative agarose gel of IS900 nested-PCR products of MAP and non-MAP strains. *IS900* nested polymerase chain reaction (*IS900* nested-PCR) goes through two rounds of PCR to amplify a 298 bp segment of the *IS900* gene that is specific for MAP. It was used to confirm the identity of clinical MAP strains **1)** UCF 3 **2)** UCF 4 **3)** UCF 5 **4)** UCF 7 **5)** UCF 8 **8)** MAP Linda and **9)** MAP Para 18. Other non-MAP strains do not have the *IS900* gene in their genome and therefore did not show any amplicons. These non-MAP strains belong to other mycobacterial species such as *Mycobacterium avium* strains **6)** JF 7 **7)** JF, **12)** *avium*; *Mycobacterium avium intracellulari* strain **10)** LM1A; and **11)** *Mycobacterium tuberculosis*.

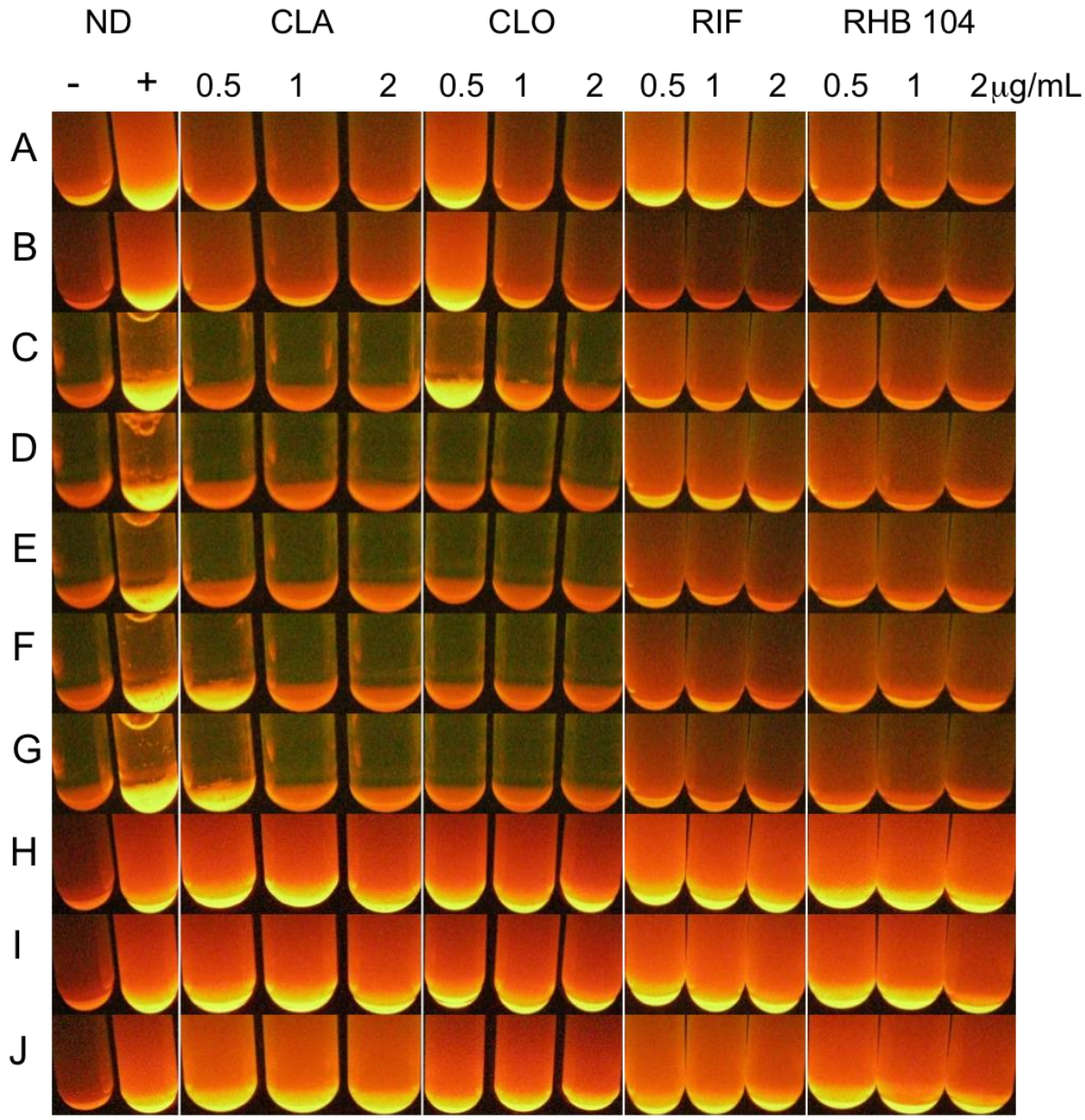

Figure 4: Potency of four antibiotic drugs against clinical MAP and non-MAP strains in vitro is shown using fluorescence quenching method. Fluorescence in the tube indicates the presence of actively respiring bacteria and an absence of fluorescence indicates bacterial growth inhibition. Seven clinical MAP strains **A)** MAP Kay, **B)** MAP Linda, **C)** UCF 3, **D)** UCF 4, **E)** UCF 5, **F)** UCF 7, and **G)** UCF 8 showed susceptibility against Clarithromycin (CLA), Clofazimine (CLO), Rifabutin (RIF), and RHB 104 at <1 μg/mL for each drug. In contrast, non-MAP strains **H)** *M. avium*, **I)** *M. avium intracellulari* LM1A, and **J)** *M. Smegmatis* showed resistance to all four drugs at 2 μg/mL. A negative control (-) with no drug (ND) and no bacteria, and a positive control (+) with ND and the same amount of inoculum were established.

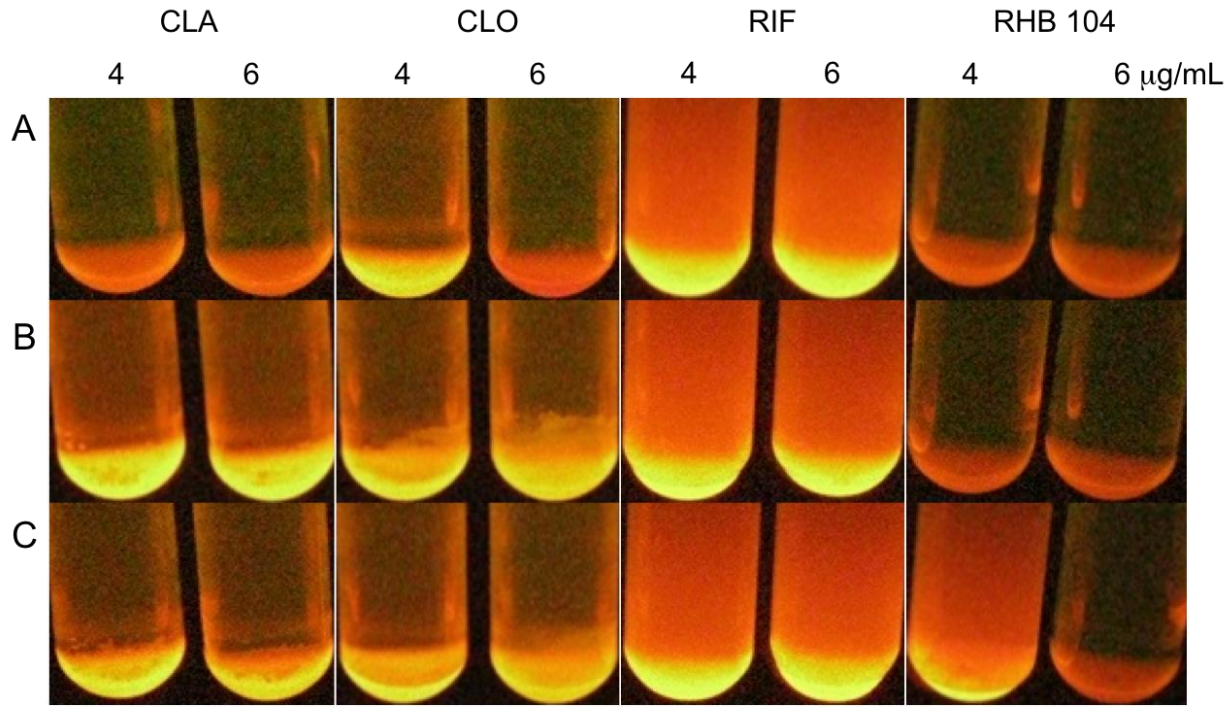

Figure 5: Resistant non-MAP strains were inhibited at higher concentrations of four antibiotic drugs. Using fluorescence quenching method, the effects of Clarithromycin (CLA), Clofazimine (CLO), Rifabutin (RIF), and RHB 104 were evaluated against non-MAP strains. **A)** *M. avium* was inhibited by all drugs at 4 or 6 μg/mL except RIF. Both **B)** *M. avium intracellulari* LM1A and **C)** *M. Smegmatis* were still resistant to CLA, CLO, RIF at 6 μg/mL. Interestingly, RHB 104 showed potency against **B)** and **C)** compared to the individual drugs. The concentrations of the drugs that did not inhibit bacterial growth were increased and tested up to 20 μg/mL (not shown).

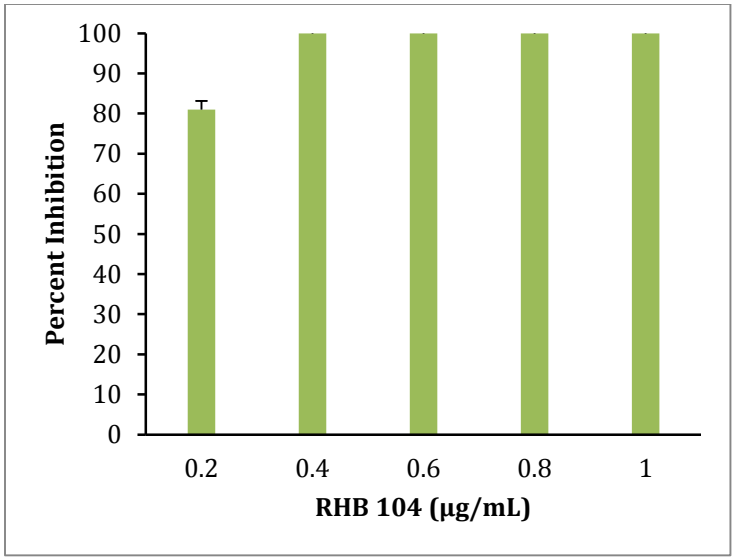

Figure 6: RHB 104 is potent at inhibiting MAP strain UCF 4 growth at low MIC levels. The bacteria were inoculated in MGIT medium with differing levels of concentration (0.2, 0.4, 0.6, 0.8, and 1 µg/mL) of RHB 104 for a period of 56 days. At 0.4 µg/mL of RHB 104, MAP strain UCF 4 was completely inhibited.

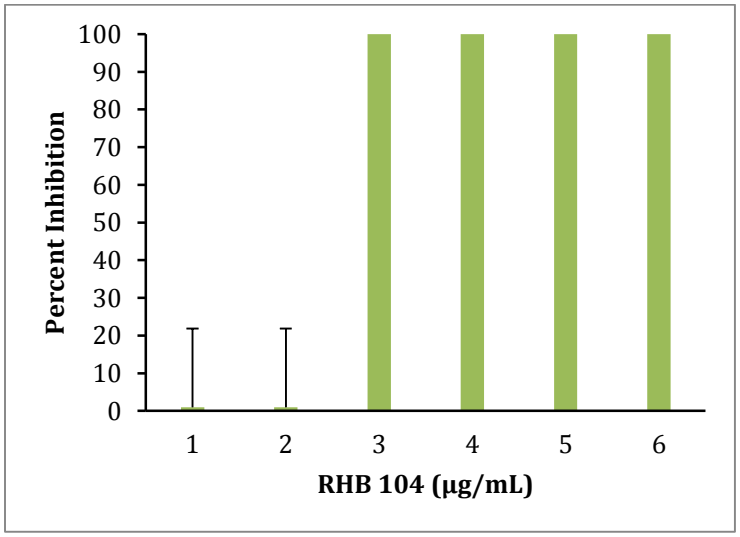

Figure 7: RHB 104 inhibits *Mycobacterium avium.* The bacteria were inoculated in MGIT medium with varying levels of concentration (1, 2 3, 4, 5, and 6 µg/mL) of RHB 104 for a period of 56 days. At a relatively high level MIC level of 3 µg/mL RHB 104, *Mycobacterium avium* was completely inhibited.

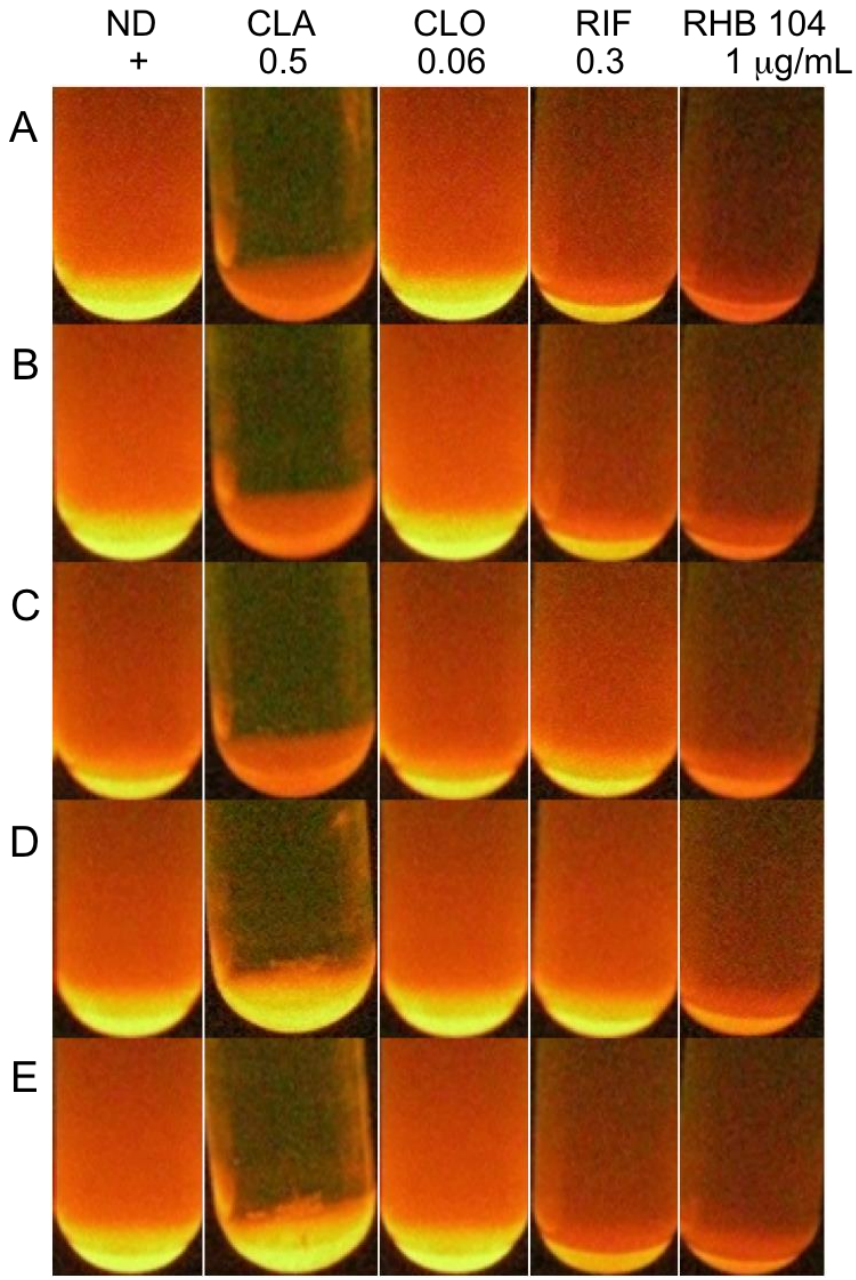

Figure 8: Clarithromycin, Clofazimine, and Rifabutin in RHB 104 showed synergistic effects against clinical MAP strains. Individually at their levels in 1 μg/mL RHB 104, CLA (0.63 μg/mL), CLO (0.06 μg/mL), and RIF (0.3 μg/mL) did not inhibit or partially inhibited growth of clinical MAP strains **A)** UCF 3, **B)** UCF 4, **C)** UCF 5, **D)** UCF 7, and **E)** UCF 8. In contrast, RHB 104 completely inhibited growth, thus showing a synergistic effect between the 3 drugs even at low dosages. A positive control with no drug (ND) was established.

Table 1: In-vitro activity of RHB 104, Clarithromycin, Clofazimine, and Rifabutin against clinical Mycobacterium strains

	MIC (µg/ml)				Comparison Analysis					
					CLA (63.3%)		CLO (6.7%)		RIF (30%)	
Organism	CLA	CLO	RIF	RHB 104	µg/ml	Suscep	µg/ml	Suscep	µg/ml	Suscep
MAP UCF 3	<1	<1	<1	<1	0.633	**S**	0.067	**R**	0.3	**R**
MAP UCF 4	<1	<1	<1	<1	0.633	**S**	0.067	**R**	0.3	**R**
MAP UCF 5	<1	<1	<1	<1	0.633	**S**	0.067	**R**	0.3	**R**
MAP UCF 7	<1	<1	<1	<1	0.633	**R**	0.067	**R**	0.3	**R**
MAP UCF 8	<1	<1	<1	<1	0.633	**R**	0.067	**R**	0.3	**R**
MAP UCF 10	ND	ND	ND	ND		**ND**		**ND**		**ND**
MAP Strain 1	<1	<1	<1	<1	0.633	**ND**	0.067	**ND**	0.3	**ND**
MAP Strain 3	<1	<1	<1	<1	0.633	**ND**	0.067	**ND**	0.3	**ND**
MAP Strain 7	<1	<1	<1	<1	0.633	**ND**	0.067	**ND**	0.3	**ND**
MAP Strain 8B	<1	<1	<1	<1	0.633	**ND**	0.067	**ND**	0.3	**ND**
MAP Ben	<1	>1	<1	<1	0.633	**ND**	0.067	**ND**	0.3	**ND**
MAP Kay	<1	<1	<2	<1	0.633	**R**	0.067	**R**	0.3	**R**
MAP Linda	<1	<1	<1	<1	0.633	**R**	0.067	**R**	0.3	**R**
MAP MS 137	<4	>6	>6	<4	2.532	**ND**	0.268	**R**	1.2	**R**
MAP MS 185	<6	<6	>6	<4	2.532	**R**	0.268	**R**	1.2	**R**
MAP Para 18	<1	>1	>1	<1	0.633	**ND**	0.067	**R**	0.3	**R**
M. avium	<4	>6	>6	<4	2.532	**R**	0.268	**R**	1.2	**R**
M. avium NEZ	>1	>1	>1	>1	0.633	**R**	0.067	**R**	0.3	**R**
M. avium JF 1	>20	>10	>20	>20	12.66	**R**	1.34	**R**	6	**R**
M. avium JF 2	>6	>6	>6	>4	2.532	**R**	0.268	**R**	1.2	**R**
M. avium JF 3	>6	>6	>6	>4	2.532	**R**	0.268	**R**	1.2	**R**
M. avium JF 4	>6	>6	>6	>4	2.532	**R**	0.268	**R**	1.2	**R**

	MIC (ug/ml)				Comparison Analysis					
					CLA (63.3%)		CLO (6.7%)		RIF (30%)	
Organism	CLA	CLO	RIF	RHB 104	µg/ml	Suscep	µg/ml	Suscep	µg/ml	Suscep
M. avium JF 5	>6	>6	>6	<4	2.532	**R**	0.268	**R**	1.2	**R**
M. avium JF 6	>6	>6	>6	<4	2.532	**R**	0.268	**R**	1.2	**R**
M. avium JF 7	>6	>6	>6	>4	2.532	**R**	0.268	**R**	1.2	**R**
M. avium JF 8	>6	>6	>6	<4	2.532	**R**	0.268	**R**	1.2	**R**
M. intracellulare LM1-A	>6	>6	>6	<6	3.798	**R**	0.402	**R**	1.8	**R**
M-Smegmatis	>6	>6	>6	<6	3.798	**R**	0.402	**R**	1.8	**R**
M. chelonae	>10	<10	>10	>10	6.33	**R**	0.67	**R**	3	**R**
M. fortuitum	>10	>10	>10	>10	6.33	**R**	0.67	**R**	3	**R**
M. scrofulaceum	<10	<10	<10	<10	6.33	**ND**	0.67	**ND**	3	**ND**
M. terrae	<10	<10	<10	<10	6.33	**ND**	0.67	**ND**	3	**ND**
M. tuberculosis	<10	<10	<10	<10	6.33	**ND**	0.67	**ND**	3	**ND**
M. xenopi	<10	<10	<10	<10	6.33	**ND**	0.67	**ND**	3	**ND**
M. vallae	<10	<10	<10	<10	6.33	**ND**	0.67	**ND**	3	**ND**

Legend: ND – not determined, R – resistance, S – susceptibility; CLA – Clarithromycin, CLO – Clofazimine, RIF – Rifabutin, MIC – minimum inhibitory concentration

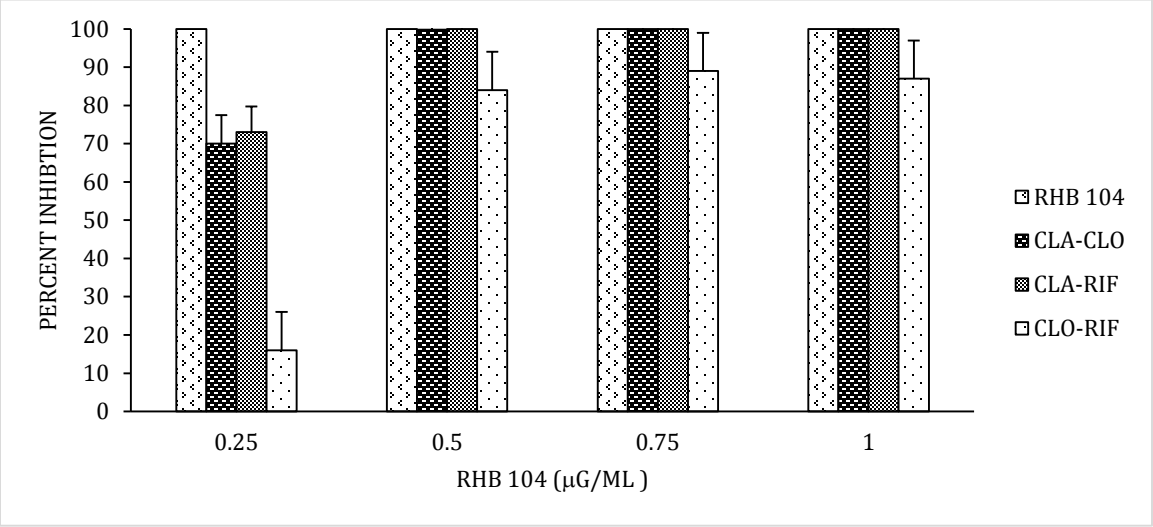

Figure 9: Two-drug combinations showed less potency of bacterial growth inhibition than RHB 104. A combination of CLA-CLO, CLA-RIF, and CLO-RIF at their levels in (0.25, 0.5, 0.75, and 1 μg/mL) of RHB 104 were tested against clinical MAP strain UCF 4. RHB 104 showed effective bacterial growth inhibition at a low MIC level of 0.25 μg/mL, whereas the 2-drug combinations showed only partial inhibition.

Table 2: In-vitro activity of 2-drug combinations in RHB 104 for their synergistic effects against MAP strain UCF 4

	MIC (μg/ml)			
	Individually	In Combination		Percent Inhibition
Antibiotic Drugs		A*	B*	(%)
CLA	0.5			100
RIF	0.5			100
CLO	0.5			100
CLA + CLO		0.32	0.03	100
CLA + RIF		0.32	0.15	100
CLO + RIF		0.07	0.3	86

Legend: *A and B are the 2 drugs in combination as written in the first column.

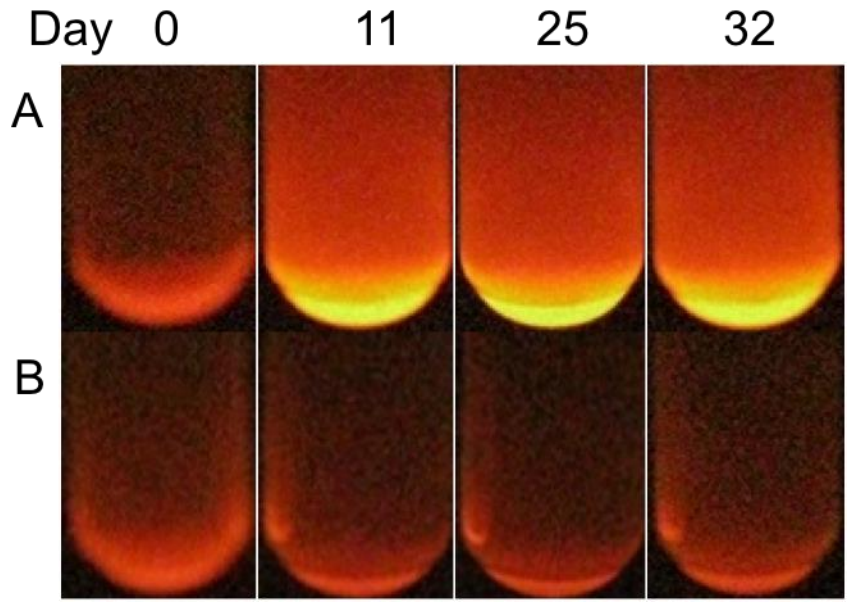

Figure 10: RHB 104 showed bactericidal activity against clinical MAP strain UCF 8. Bacteria were harvested from a previous RHB 104 drug susceptibility experiment MGIT culture. MAP strain UCF 8 from a previous positive control with no drug was washed and **A)** re-inoculated in a fresh MGIT medium. Another MAP strain UCF 8 from a culture with 1 μg/mL of RHB 104 that showed no fluorescence under the UV light was washed and **B)** re-inoculated in a fresh MGIT medium with no drugs. After 32 days, **A)** positive control was fluorescent, showing presence of actively respiring bacteria, whereas **B)** showed fluorescence quenching.

CHAPTER THREE: DEVELOPMENT OF MULTICOLOR *IN-SITU* HYBRIDIZATION TECHNIQUE FOR DETECTION OF PATHOGENS FROM INTESTINAL MUCOSA OF CROHN'S DISEASE PATIENTS

Opportunistic pathogens *Mycobacterium avium* subspecies *paratuberculosis* (MAP) and adherent invasive *Escherichia coli* (AIEC) have each been implicated as the causative agent in Crohn's Disease (CD), a chronic granulomatous inflammatory bowel disease in humans[7, 9, 72]. Although extensive studies have investigated the presence of MAP or AIEC in CD patients, only one recent study conducted by Nazareth et al investigated the two pathogens simultaneously in both CD and non-CD individuals[10]. Both MAP and AIEC were detected in the peripheral blood of CD patients using polymerase chain reaction (PCR). They were both found to have higher prevalence among CD patients as opposed to non-CD patients, leading to a possible conjoined causation. Even so, these two pathogens have not been studied simultaneously in affected intestinal tissues of CD patients.

MAP has long been associated with CD. In 1913, a surgeon named Thomas Dalziel first proposed a mycobacterial causation of CD after identifying pathophysiological similarities between Crohn's disease (then called chronic interstitial enteritis in humans) and Johne's disease (JD), an inflammatory bowel disease in cattle[73]. JD is caused by MAP, a ubiquitous, acid-fast and mycobactin-dependent bacillus. MAP was isolated from affected intestinal tissues of two CD patients[7]; however, these isolates were found to be cell-wall deficient (CWD) and a simple Ziehl-Neelsen acid fast stain yielded negative results[74]. In addition, because of its CWD-form, isolating MAP from tissue samples and culturing it *in vitro* became a hurdle in identifying its presence in CD patients. Although the development of a liquid medium containing mycobactin J enabled culturing of MAP *in vitro,* MAP can still take 8 weeks to 6 months to grow. The development of

nested PCR technique enabled identifying MAP from samples instantaneously prior to or concurrent with culturing. Using *IS900* nested PCR, a 298 base pair segment of the *IS900* gene in MAP DNA is amplified[9]; this gene is specific for MAP and has 15-18 copies in the entire genome. With these newer techniques, further evidence has shown the presence of MAP DNA in the mesenteric lymph nodes, breast milk, and peripheral blood of CD patients[6, 9, 10, 74-81]. The MAP CWD form has also been found in affected tissues by in-situ hybridization[34, 82, 83].

MAP is an obligate, intracellular pathogen that evades the immune system by sequestering itself inside phagocytic cells such as macrophages and dendritic cells[84, 85]. MAP persistence within these cells is attributed to their ability to inhibit the fusion of phagosome and lysosome[84, 86, 87]. Phagocytic cells reside in the lamina propria of the intestines where they act as secondary defense to invading pathogens such as MAP that penetrate the intestinal epithelial layer[88]. Similarly, AIEC has been shown to enter epithelial intestinal tissues through a macropinocytosis-like process[89, 90]. As they traverse the epithelial cells, phagocytic cells in the lamina propria, especially macrophages, take them up. AIEC resides in vacuoles inside the macrophages, and can also persist in the cytoplasm[91]. The successful invasion of macrophages by AIEC is similar to that of MAP. AIEC prevents the phagolysosome fusion and the acidification of phagosome. Their survival inside the macrophages enables AIEC to exponentially grow within 48 hours of phagocytic cell invasion[89].

AIEC, specifically strain LF82, has been linked to CD after its isolation from the ileal lesion of a CD patient[12, 91]. It has also been detected from the peripheral blood, intestinal mucosa, and lymph nodes of CD patients[10, 12, 14, 92-94]. Genomic studies have shown that AIEC belongs to the B2 phylogenetic group, which usually categorizes extraintestinal *E. coli* that utilizes the type IV secretion system[95, 96]. Although AIEC has been associated with CD, several strains isolated from patients with ulcerative colitis showed indistinguishable genetic makeup with AIEC from

patients with CD[96]. This poses the question of causality of AIEC to CD or secondary to an underlying causation, thus, a direct method of visualizing its presence in differing stages of CD might provide clues as to its role in CD pathogenesis.

The advent of *in-situ* hybridization technique in 1969 paved way for analysis of chromosomes and cytological components[97, 98] by visualization using radioactive materials. This technique was further developed by using very stable fluorescent molecules for fluorescent *in situ* hybridization (FISH) of RNA-DNA hybrids[99]. FISH is used in many clinical applications, extending from diagnosing genetic diseases[100] to identifying pathogens that cannot be cultured *in vitro* such as *Mycobacterium leprae* in lepromatous leprosy[101]. By using oligonucleotide probes, target species such as MAP or AIEC can be identified from CD patient intestinal tissues with great sensitivity using FISH, bypassing the limitations of culturing method and contaminations of PCR[102]. In addition, PCR amplifies any DNA, whether it is remnant, circulating, non-infectious DNA or DNA extracted from a viable, infectious microorganism. The misleading amplification of DNA can lead to contradicting PCR results, as is reported in numerous studies. FISH enables detection of DNA only from viable, infectious MAP and/or AIEC in the intestinal mucosa, specifically pinpointing the involved pathogens at the site of inflammation. We have previously shown using FISH that MAP is present in some CD patients[34]. Another report showed an invasive type of *Escherichia coli* to be present in the ileal mucosa of CD patients using FISH but not in healthy controls[103]. These separate, individual evidences further augmented the on-going debate about which pathogen is the actual causative agent of Crohn's Disease or if it is a multifactorial causation involving multiple pathogens.

This study is aimed to develop a multicolor detection method using FISH to simultaneously detect these two pathogens from intestinal tissue samples of CD and non-CD patients. This

optimized method will help 1) determine the presence and prevalence of both MAP and AIEC in affected intestinal tissues of CD patients, and 2) determine the spatial distribution of both pathogens in affected intestinal tissues. Based on evidence from previous studies, we hypothesized both pathogens to be present in tissue samples, with MAP being more prevalent in CD patients.

Materials and Methods

Bacterial Strains

MAP strain UCF 4 and *E.coli* strain K-12 (ATCC 33625) were used for development and optimization of the protocol. Commensal, non-pathogenic EC (npEC) is expected in the gut, and was used as a control. There was no AIEC culture obtained for this project; therefore, npEC was used as a negative control against the AIEC probe. MAP was thawed out from -80°C freezer and was cultured in BD Bactec™ MGIT™ Para-TB medium with 800 µL growth supplement. In order to prevent clustering of MAP in culture, 0.1% Tween 80 (Acros Organics, New Jersey) was added to the culture medium. During the exponential phase, 1 mL of MAP was removed from culture using aseptic technique. It was centrifuged at 13,200 rpm for 2 minutes, and washed in TE buffer. The supernatant was discarded, and the pellet was re-suspended in 500 µL of TE buffer. A volume of 20 µL was smeared on each glass slide, air-dried, and heat fixed. *E. coli* strain K-12 was also thawed out from -80°C freezer. It was grown on a nutrient agar plate and incubated at 37°C. After visible growth on the culture plate, one colony was removed using aseptic technique and re-suspended in 500 µL of TE buffer. Glass slides were smeared with 20 µL of npEC. They were air-dried, heat fixed, and stored until further use. Acid fast and gram stain were used to confirm the presence on the glass slide of MAP and npEC, respectively.

Tissue Samples

The intestinal mucosal tissue samples used in this study were obtained from tissue collections bank in Dr. Naser's lab. All clinical samples were received following UCF Internal Review Board (IRB) approval. Demographic data were collected but nothing related to patient's contact information. Clinical samples were not collected from patients for this study; instead, samples were collected for non-related diagnostic or therapeutic purposes. These samples embedded in paraffin wax were taken from the -80°C. Sequential cuts of 3 μm sections for each tissue were placed on 10 glass slides. Each tissue samples was given a code to identify patient demographics at the conclusion of this blind study (Table 4).

Preparation of oligonucleotide probes

The probes for MAP, AIEC, and npEC were adapted from previous studies with a few modifications (Table 3)[104, 105]. The amine-modified oligonucleotides were dissolved in DNAse-free water to achieve a final concentration of 25 μg/μL. The oligonucleotide stock solution was stored at -20°C for further use. The reactive dyes were dissolved in 14 μL of DMSO per 250 μg and stored at -20°C until further used. A reaction mixture of 7 μL of deionized water, 75 μL of labeling buffer (0.1 M sodium tetraborate buffer, pH 8.5), 4 μL of a 25 μg/μL oligonucleotide stock solution and 14 μL of reactive dye in DMSO was added to a vial and incubated overnight at room temperature on an oscillating shaker. After 24-hours, 10 μL of 3M NaCl and 250 μL of cold absolute ethanol were added to the reaction vial and incubated at -20°C for 30 minutes. The reaction mixture was centrifuge at 11,400 rpm (12,000 x g) for 30 minutes. The supernatant was removed and the pellet was washed with 70% ethanol. The pellet was dried briefly, and was

dissolved in 100 µL TE buffer (stock concentration of 1 µg/µl). The purified oligonucleotide-labeled probe was stored at -20°C for further use.

Table 3: Oligonucleotide Probes for MAP, pathogenic E. coli, and non-pathogenic E. coli

Organism	Oligonucleotide Sequence	Specificity	Probe	Fluorophore
MAP	ATG TGG TTG CTG TGT TGG ATG G[9]	*IS900*	MAP488	AF 488
AIEC	GCA AAG GTA TTA ACT TTA CTC CC[105]	16s rRNA	AIEC546	AF 546
npEC	CAT GCC GCG TGT ATG AAG AA	16s rRNA	EC647	AF 647

Legend: MAP – *Mycobacterium avium* ss. *paratuberculosis*, AIEC – adherent-invasive *Escherichia coli*, npEC – non-pathogenic *Escherichia coli*, AF – Alexa Fluor.

Bacterial Fixation

The FISH protocol was adapted from our previous study with some changes[34]. Briefly, bacteria were fixed with 4% paraformaldehyde for 30 minutes at room temperature (RT). After fixation, they were washed three times in 1X PBS (pH 6.8) for 10 minutes each. The bacterial membranes were permeabilized in 100 µL of 1% SDS and 20 µg/mL of Proteinase K at 55°C for 30 minutes. The enzyme was inactivated using 0.2% glycine for 3 minutes at RT. Bacterial slides were washed as stated above. They were dehydrated with 50%, 80%, and 100% ethanol washes for 1 minute each. Bacterial slides were washed in xylene for 1 minute to remove excess lipids before going through another round of 100%, 80%, and 50% ethanol washes for 1 minute each. Lastly, they were incubated in 1X PBS (pH 6.8) for 1 hour at RT.

Bacterial Fluorescent In-situ Hybridization

For each bacterial slide, a mixture containing 20 µL of hybridization solution (1% Triton X100, 2X SSC, 500 µg/ml denatured sperm DNA, 10% dextran sulfate, 50% deionized formamide and water) with 100 ng oligonucleotide probe was boiled for 10 minutes and displaced on ice for

another 10 minutes. Prior to hybridization, bacterial slides were incubated in a pre-hybridization buffer (2X SSC, 20% dextran sulfate, 50% formamide, and water) for 5 minutes at 50°C. The bacterial slides were transferred in a hybridization chamber. The hybridization mixture was added on to the slides for an overnight incubation at 37°C. After 24-hours, the slides were washed on a shaker for 15 minutes each with 2X SSC (RT), 1X SSC (RT), 0.3X SSC (40°C), and 0.3X SSC (RT). Slides were further washed with diH_2O three times for 10 minutes each at RT, and allowed to air dry in the dark. Slides were mounted with anti-photobleaching medium (Vector Laboratories, Burlingame, CA).

Fluorescent In-situ Hybridization on Intestinal Tissue Samples of CD Patients

The tissues were de-paraffinized in three washes of xylene each for 10 minutes. They were then washed for 10 minutes each in 100%, 80%, and 50% ethanol. The tissues were incubated in 1X PBS (pH 6.8) for 5 minutes and air-dried. A cocktail solution of 20 μL hybridization buffer and 1 μL oligonucleotide probe per slide were mixed and added on to the dried tissue slides. The slides were covered in parafilm and transferred in to hybridization chambers. They were incubated at 55°C for 90 minutes. After hybridization, the slides were washed for 15 minutes in 2X SSC (RT), 1X SSC (RT), 0.3X SSC (40°C), and 0.3X SSC (RT). The three final washes for the slides were in diH_2O at RT for 10 minutes each. The slides were air-dried in a dark room. One drop of mounting medium with DAPI (Vector Laboratories, Inc. Burlingame, CA) was spotted on the tissue. The slide was covered with a cover slip and sealed with clear nail polish.

Analysis

The cultured bacterial slides and tissues slides were analyzed using confocal scanning laser microscopy (CSLM). The signals were detected through each respective channel at wavelengths of 488 nm, 546 nm, and 647 nm. The images for each bacterial slides were taken at a total magnification of 1000-1500x and the images for tissue slides were taken at a total magnification of 630-945x. The signals detected were analyzed together using ImageJ 1.49v (National Institutes of Health, USA).

Results

Specificity of each oligonucleotide probe

The sequences for MAP, AIEC, and npEC were analyzed using BLAST. The antisense strands were determined as shown in Table 3. The non-pathogenic EC probe sequence has a 100% identity (E-value: 5e-04) with the 16s rRNA of EC strain K-12 (Figure 11). The MAP probe sequence has a 100% identity (E-value: 8e-06) with the *IS900* sequence of MAP (Figure 11). Lastly, the AIEC probe sequence has a 100% identity (E-value: 7e-07) with the 16s ribosomal RNA (rRNA) of AIEC strain LF82 (Figure 11). In addition, the AIEC probe sequence is also showing specificity against npEC strain (E-value: 1e-05).

FISHing for cultured MAP and npEC

Suspensions of cultured MAP and npEC were each smeared on separate glass slides and were targeted using the specific probes MAP488 and EC647, respectively. Under CSLM analysis, the emission signal at 647 nm (red) was detected from the npEC slides (Figure 12), and at 488 nm (green) from the MAP slides (Figure 13). The specificity of the probes to each respective bacterial

target was also tested. EC647 probe was used against cultured MAP and MAP488 probe was used against cultured npEC. There were no signals detected under the CSLM from neither cultured npEC nor cultured MAP, showing probe specificity (image not shown).

FISHing for AIEC

There was no cultured AIEC acquired for this project. The probe specificity for AIEC (AIEC546) was tested against the cultured EC strain K-12, thus serving as the negative control. Under CSLM analysis, no signals were detected at 546 nm wavelength (Figure 14), confirming that the probe is specific only to AIEC and not to commensal *Escherichia coli*.

FISHing for MAP, AIEC, and npEC on Intestinal Mucosa

A total of 9 tissue samples from the intestinal mucosa of CD patients were used for the experiments (Table 4). In 6 tissue samples (Figure 15), red signals (647 nm) were detected under the CSLM, indicating the presence of npEC in the intestinal mucosa of CD patients. In 6 other tissue samples (Figure 16), green signals (488 nm) were detected under the CSLM, indicating the presence of MAP in the lamina propria of the intestines. AIEC was also detected sparingly in 3 other tissue samples (Figure 17) from CD patients. In 2/9 tissue samples, all three bacteria were detected individually using each oligonucleotide probe. These probes individually were able to target the respective bacteria npEC, MAP, and AIEC, showing the localization of each bacterium within the lamina propria of the intestinal tissues of CD patients.

Dual-FISH on tissue samples

Following the aforementioned results, a cocktail of two oligonucleotide probes were mixed: (i) MAP and npEC probes (Figure 18), (ii) MAP and AIEC probes (image not shown), and (iii) npEC and AIEC probes (image not shown). The dual probe cocktails were used to target each respective bacterium in the intestinal tissue samples of CD patients. In Figure 18, the use of both MAP and npEC oligonucleotide probes showed the presence of both bacteria in the intestinal mucosa. This simultaneous detection enabled identification of the spatial distribution of each bacterium in the intestinal mucosa. In some areas, there was an overlap of signals, which could be from co-localization of these bacteria.

Discussion

A bacterial etiology of Crohn's Disease has been extensively studied after the isolation of opportunistic pathogens MAP or AIEC from CD patients. However, a causative agent of CD has not been established due to conflicting results[106-110]. A previous study has detected both intracellular pathogens simultaneously from the peripheral blood of CD patients but these pathogens have not been detected from affected intestinal tissues[10]. The aim of this study was to develop a multicolor imaging technique using fluorescent *in-situ* hybridization to detect MAP and AIEC simultaneously in order to determine the presence and spatial distribution of MAP and AIEC from the intestinal mucosa of CD patients. This study presented an optimized technique using FISH to (i) detect cultured MAP and npEC *in vitro* and (ii) detect MAP, AIEC, and npEC *in situ* from the intestinal mucosa of CD patients.

Initially, we have optimized a protocol that enables detection of MAP and npEC from culture using oligonucleotide probes and FISH. In this study, npEC was used as a negative control

against AIEC and it was also used to show that npEC is present in human intestinal tissue samples as expected. The labeled oligonucleotide probes were shown to bind to their targeted bacteria, MAP or npEC. The specificity of the oligonucleotide probes was further tested by using MAP probe against npEC, and npEC probe against MAP. The absence of signals showed that the oligonucleotide probes only bind to their respective bacterial target. Although AIEC was not cultured and used in this experiment, the specificity of labeled oligonucleotide probe, which sequence was adapted from a previous study[105], was used against npEC. The absence of the signal from npEC showed that the oligonucleotide probe only binds to AIEC. This is beneficial in delineating the difference between npEC and adherent invasive EC. As a result, we developed a protocol for FISH using oligonucleotide probes and optimized it using cultured bacteria to simultaneously detect MAP and npEC.

Further optimization of the protocol was needed to work with intestinal mucosa of CD patients. Initially, the probes were used individually to detect MAP, AIEC, or npEC from tissue samples. All of the tissue samples tested showed the presence of npEC as expected. Both MAP and AIEC were also detected individually from the intestinal tissue samples of CD patients, specifically in the lamina propria. MAP was detected in its almost spherical form, as we have shown previously[9]. These results led to combination of probes in a cocktail solution to achieve the goal of the study, a multicolor detection method. Using the optimized protocol, simultaneous detection of MAP and EC, MAP and AIEC, or AIEC and EC from the tissue samples were achieved. An overlay of the images showed that there might be co-localization of some of these bacteria in the lamina propria of the intestinal mucosal samples. It was not surprising to see a possible co-localization of these bacteria in the lamina propria of the intestines because of the resident macrophages that phagocytize invading microorganisms.

Although the optimized protocol detected the presence of MAP, npEC, and AIEC both from culture and in intestinal tissue samples, there were a few limitations to this study. Positive controls for the AIEC oligonucleotide probe must be establish to determine its specificity and sensitivity in targeting only AIEC while discriminating against npEC. Additionally, further studies can be done to confirm the detected signals for MAP, npEC, and AIEC using labeled antibodies specific for each bacterium. An important addition to this validation is to identify phagocytic cells within the lamina propria to determine the actual spatial distribution of each bacterium.

Overall, a protocol using fluorescent *in situ* hybridization method was developed and optimized to target MAP, npEC, and AIEC from cultured microorganisms as well as tissue samples from CD patients. This method can be applied to a larger sample size to determine the presence and role of MAP and AIEC in different stages of Crohn's Disease. Additionally, other pathogens such as *Listeria monocytogenes*, *Klebsiella pneumonia*, and *Clostridium difficile* have also been associated with Crohn's Disease. This FISH protocol can be applied for a multiple detection of all these pathogens to determine which of them is the causative agent of CD. It may also be interesting to find out whether CD is a chronic disease that is caused by one pathogen such as MAP or AIEC, or it is caused by multiple pathogens.

Table 4: Intestinal Tissue samples from Crohn's Disease patients.

Patient #	Age	Sex	Ethnicity	Family Hx of IBD	Diagnosis	Site of Tissue Sample	npEC	MAP	AIEC
NLF-1745	30	F	C	N/A	CD	N/A	X		
NLF-1036	23	M	Unknown	N/A	CD	N/A			
NLF-1637	31	F	Unknown	N/A	CD	N/A			
NLF-2800	51	M	Unknown	N/A	CD	N/A	X		
NLF-2963	28	F	C	Brother: CD	CD	N/A			
NLF-3115	34	M	C	N/A	CD	Right colon			
NLF-3127	38	F	C	N/A	CD	Transverse colon	X		
NLF-0014	31	M	C	N/A	CD	N/A			
NLF-1040	26	F	AA	N/A	CD	N/A		X	
NLF-1130	48	F	C	N/A	CD	Rectum	X	X	
NLF-0145	27	F	AA	N/A	CD	N/A	X	X	X
NLF-1624	49	M	H	N/A	CD	N/A			
NLF-1703	31	F	AA	Father: IBD	CD	N/A			
NLF-1780	22	F	H	N/A	CD	N/A		X	
NLF-2313	50	M	H	N/A	CD	N/A			
NLF-2446	50	M	AA	N/A	CD	N/A			
NLF-0268	63	F	Unknown	N/A	CD	Ascending colon	X	X	X
NLF-0597	31	F	C	N/A	CD	Ileum		X	X
NLF-0656	63	F	H	N/A	CD	N/A			

Legend: F – female, M – male, C – Caucasian, AA – African American, H – Hispanic, N/A – not applicable, CD – Crohn's Disease, IBD – inflammatory bowel disease

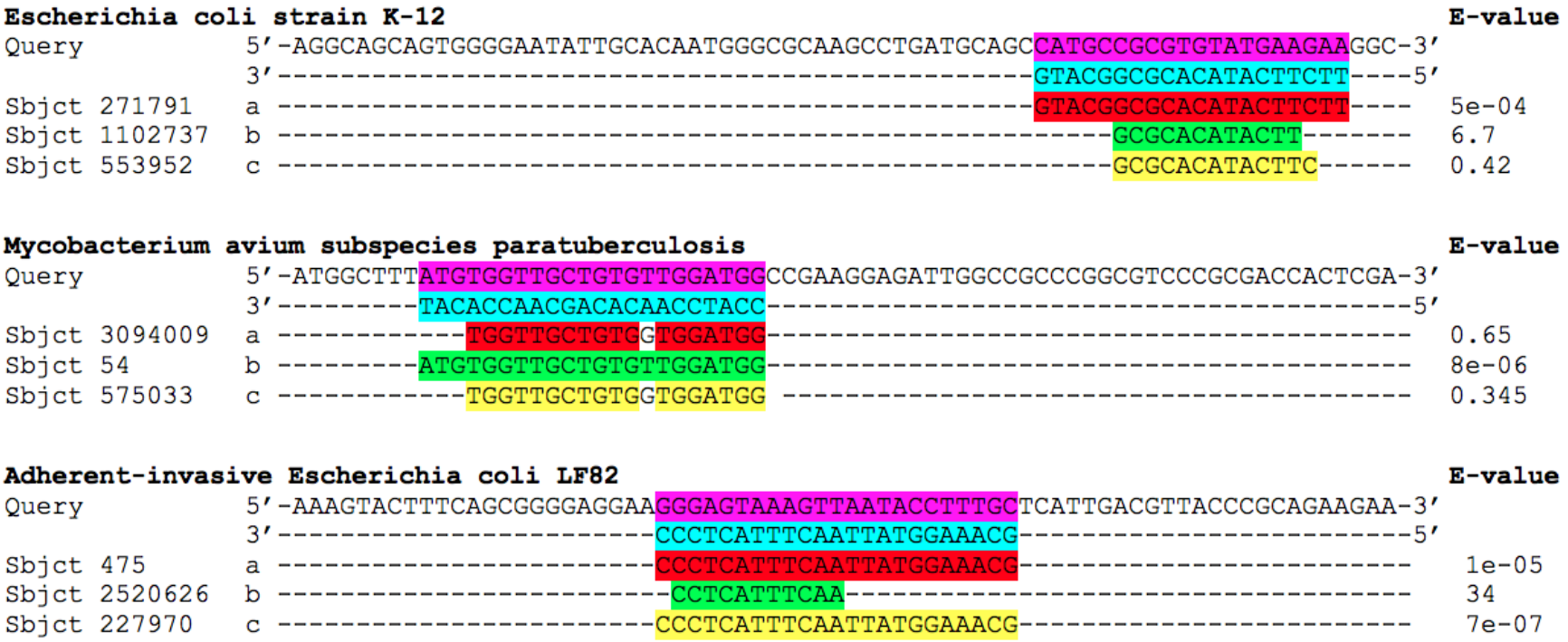

Figure 11: BLAST analysis of the oligonucleotide probes for non-pathogenic EC, MAP, and AIEC. The 16s rRNA sequence for the non-pathogenic *E.coli* probe was analyzed against **b)** MAP (green) and **c)** AIEC (yellow) genome, whereby showing the probe is specific for non-pathogenic *E. coli.* The *IS900* sequence for the MAP probe was also analyzed against **a)** non-pathogenic EC (red) and **c)** AIEC (yellow). The low e-value of the MAP probe against MAP was indicative of a more biologically related significance than that with non-pathogenic EC and AIEC, thus conferring specificity. Lastly, the AIEC probe was analyzed against **a)** non-pathogenic EC and **b)** MAP. In this instance, the probe showed biological relation with both non-pathogenic EC and AIEC, with the latter showing more specificity.

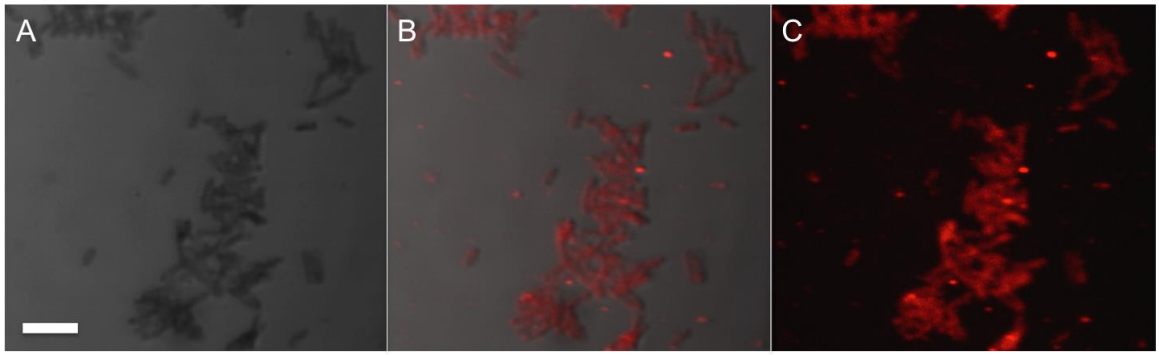

Figure 12: FISHing for non-pathogenic *E. coli* using EC647. Cultured *E. coli* grown on a nutrient agar plate was smeared and heat-fixed on a glass slide. This was used to optimize the fluorescent *in situ* hybridization (FISH) technique using the non-pathogenic *E. coli* probe EC647 to target the 16s rRNA of the non-pathogenic *E. coli*. The left panel **a)** was the differential interference contrast (DIC) image, showing bacterial structure. The right panel **c)** captured the red signal emitted from the EC647 probe bound to the target. The middle panel **b)** showed an overlay of both aforementioned images. Total magnification at 1500x. Scale bar at 10 μm.

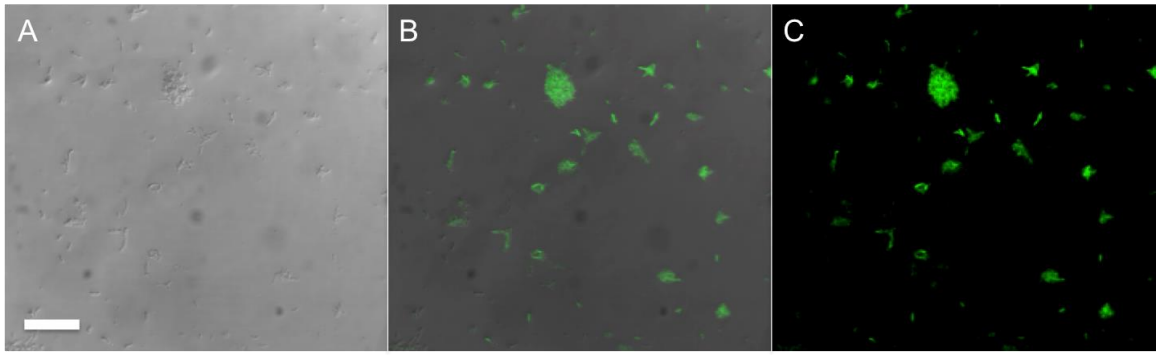

Figure 13: FISHing for *Mycobacterium avium paratuberculosis* using MAP488 probe. Cultured MAP was used to optimize the FISH technique using the MAP488 probe that targets the *IS900* sequence in the MAP DNA. The left panel **a)** showed the structural image of the bacteria, which is **b)** overlaid (middle panel) with the fluorescent green signal from the right panel **c)**. The signals correspond to the structure, showing adherence to the target by the MAP488 probe. Total magnification at 1000x. Scale bar at 10 μm.

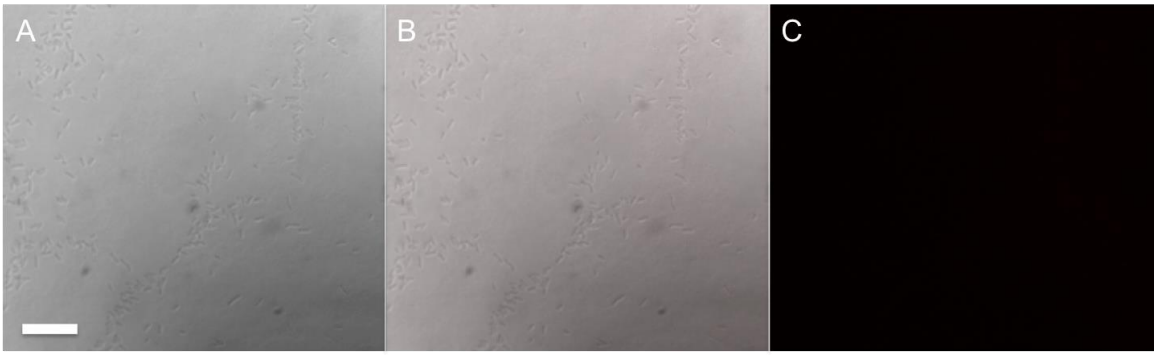

Figure 14: FISHing for non-pathogenic *E. coli* using the pathogenic probe AIEC546. Cultured non-pathogenic *E. coli* was used as a negative control to test the specificity of the pathogenic probe AIEC546. The DIC image on the left panel **a)** showed the presence of bacteria on the slide; however, **c)** no signal was emitted by the AIEC546 probe. This showed **b)** probable non-binding of the probe to the non-pathogenic *E. coli*. Total magnification at 1000x. Scale bar at 10 μm.

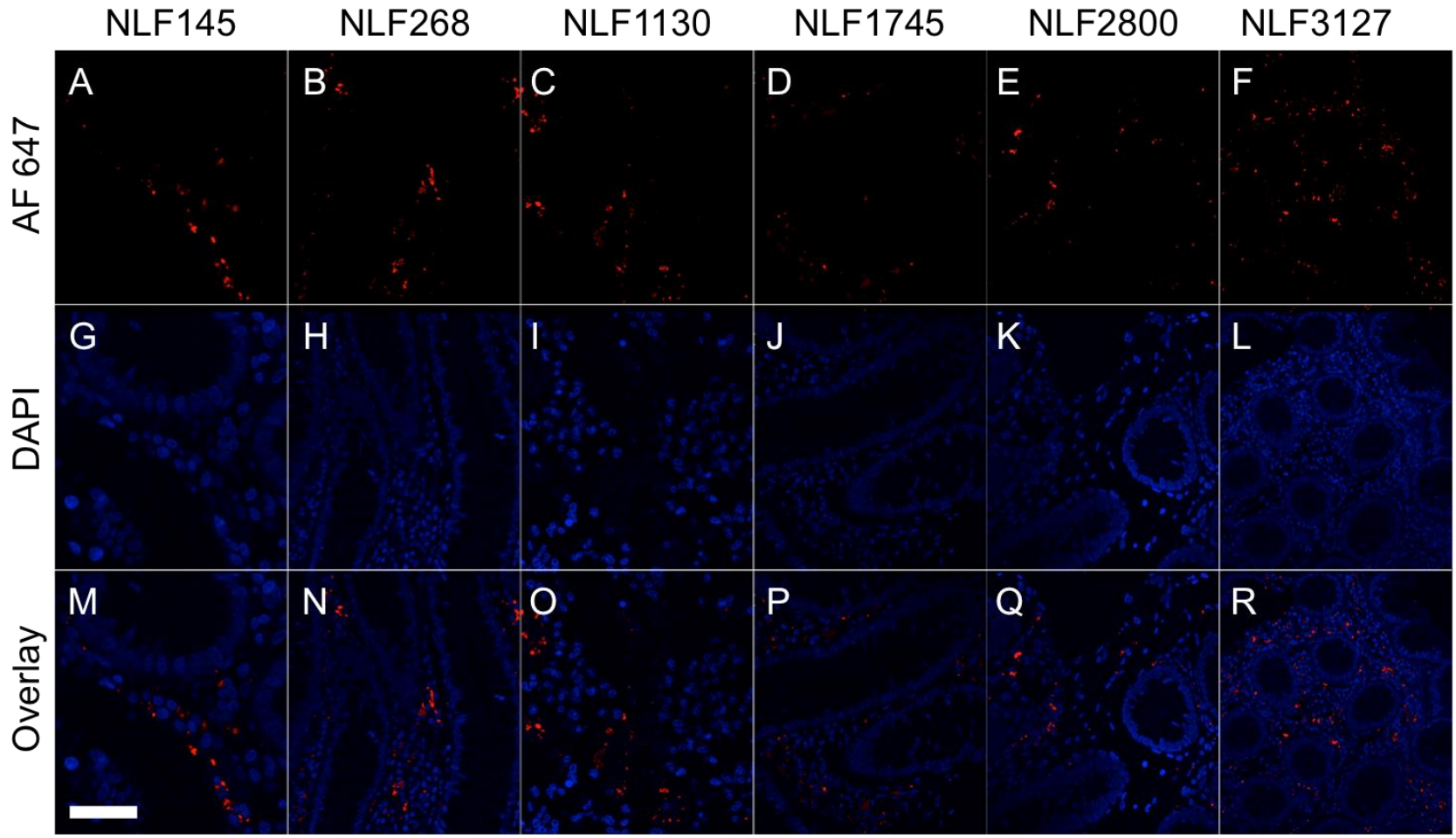

Figure 15: Non-pathogenic *E.coli* is present in the intestinal mucosa of Crohn's disease patients. In six different tissue samples from CD patients, the EC647 oligonucleotide probe was used to FISH for non-pathogenic (commensal) *E. coli*. The red signals (647 nm) in **A-F** were detected in the lamina propria for each tissue sample (**M-R**). The background tissue was stained with DAPI (**G-L**). Scale bar at 10 μm.

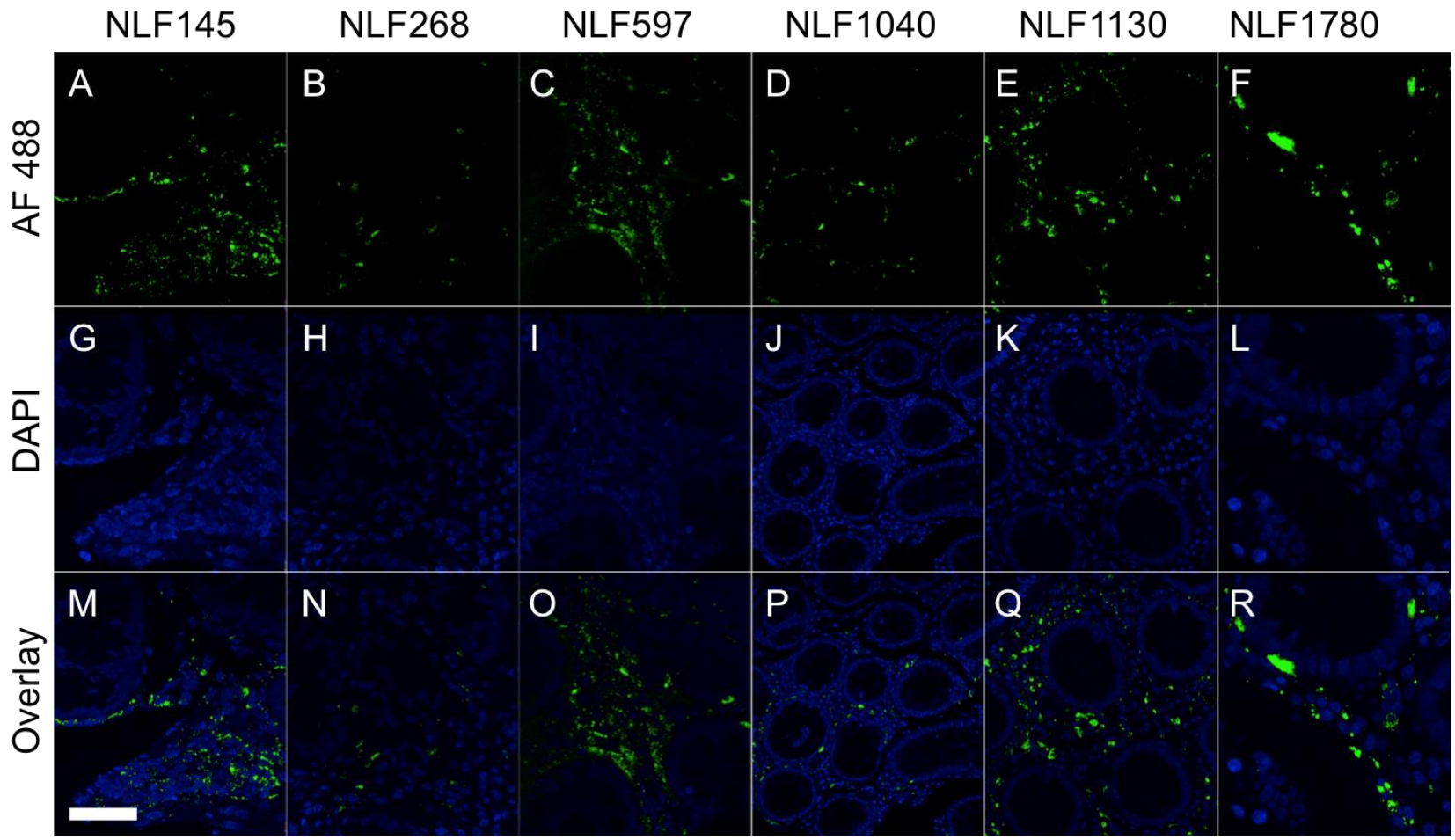

Figure 16: ***Mycobacterium avium paratuberculosis*** **penetrated the lamina propria of intestinal tissues of CD patients.** The MAP488 oligonucleotide probe was used in FISH to target MAP in the intestinal tissues of 6 CD patients. The signals (**A-F**) emitted at 488 nm were overlaid with the surrounding DAPI-stained tissues (**G-L**) showing localization of MAP within the lamina propria (**M-R**). Scale bar at 10 μm.

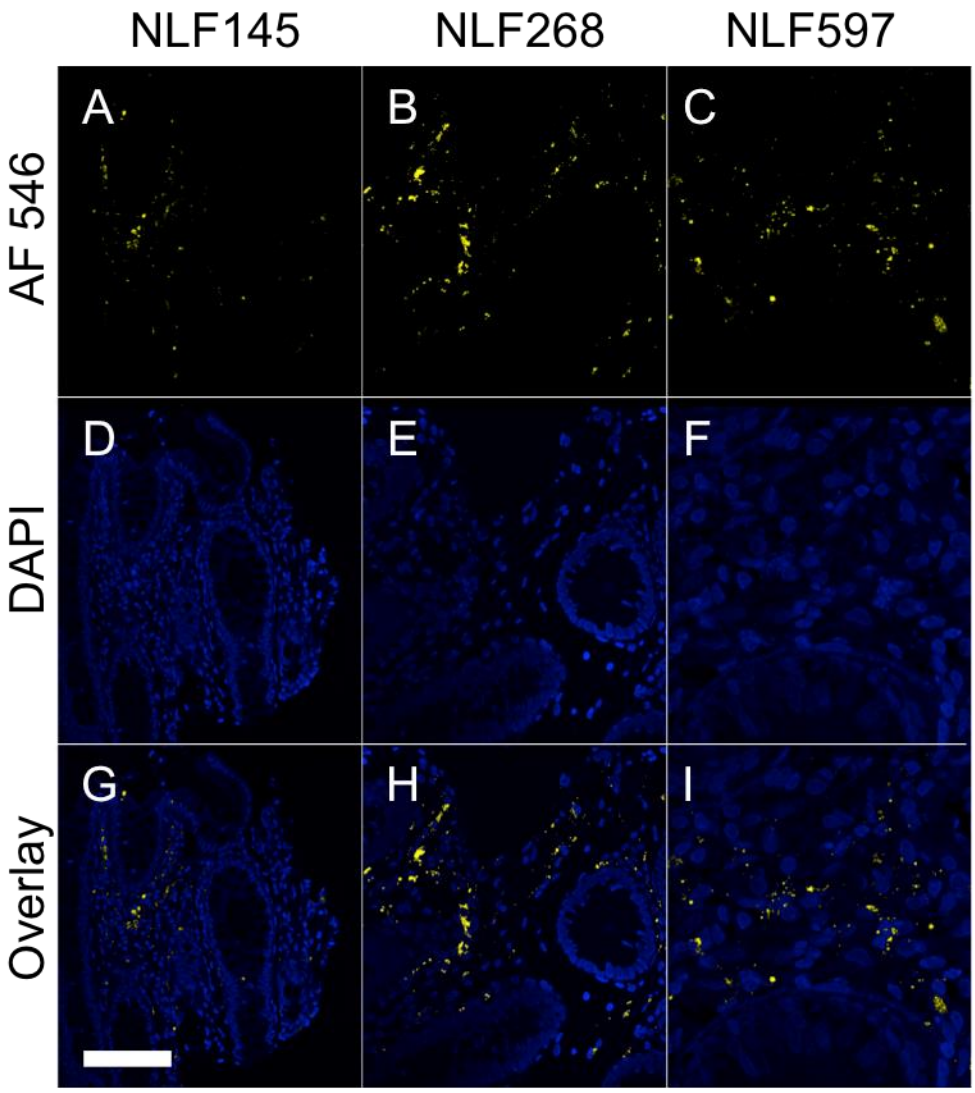

Figure 17: FISHing for adherent invasive *E. coli* in the intestinal tissues of CD patients. Using the AIEC546 oligonucleotide probe, AIEC was targeted as shown by the yellow signals emitted at 546 nm (**A-C**). Background tissues were stained with DAPI (**D-F**). AIEC, like MAP and npEC, were also localized in the lamina propria of the intestinal tissues of 3 CD patients (**G-I**). Scale bar at 10 μm.

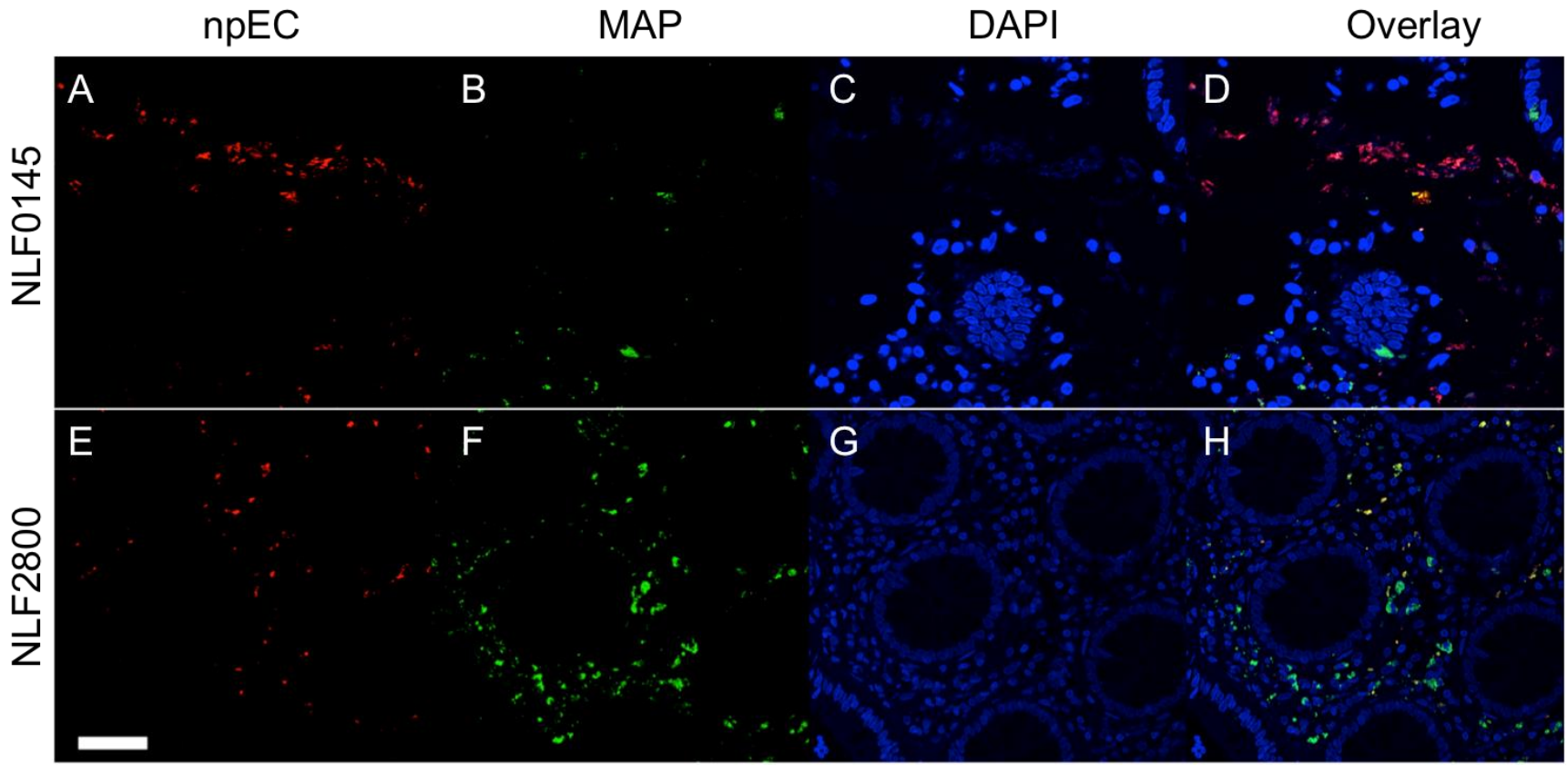

Figure 18: Dual FISHing of intestinal tissues shows bacterial presence and co-localization. In tissue samples obtained from CD patients, two oligonucleotide probes EC647 and MAP488 were used simultaneously to FISH for non-pathogenic EC (**A&E**), and MAP (**B&F**). The background tissue sample stained with DAPI (**C&G**) overlaid with the two signals (**D&H**) showed the presence of both bacteria in the lamina propria of the intestinal tissues. In some areas, there may also be co-localization of the npEC and MAP. Scale bar at 10 μm.

CHAPTER FOUR: CONCLUSION

A possible microbial causation in Crohn's Disease has long been investigated due to the individual isolation and detection of opportunistic pathogens such as *Mycobacterium avium* subspecies *paratuberculosis* and adherent-invasive *Escherichia coli*[10]. This correlation has brought about treatment options using antibiotic therapy. In this study, we determined and established the efficacy *in vitro* of a new combinatorial antibiotic drug RHB 104 against clinical MAP and non-MAP strains. In doing so, we also showed a synergism between the lowered dosages of the three drugs in RHB 104. Secondly, we detected both MAP and AIEC from the intestinal mucosa of CD patients using the multicolor fluorescent *in situ* hybridization technique that we developed as a part of the study.

We consider MAP to be a leading etiological agent for CD after isolation and detection from affected intestinal tissues, lymph nodes, peripheral blood, and breast milk of CD patients[7, 9, 10, 83]. This correlation has shaped treatment options on antibiotic drugs, specifically Clarithromycin, Rifabutin, and Clofazimine. This combination was used in previous studies resulting in varying results, possibly attributed to the high drug dosages administered over a long period of treatment[4]. In contrast, a patient who suffered severe recurring CD, and who have utilized all source of treatment from surgical to pharmacological successful treatment was successfully cured with no relapse after treatment with this drug combination[11]. In RHB 104, the dosages of these three drugs were lowered. Our findings confirmed that despite the low dosages in RHB 104, it is still efficacious against clinical MAP and non-MAP strains. This finding is more important in that, RHB 104 is more potent against clinical MAP strains as shown by the lower MIC for RHB 104 than in their counterpart non-MAP strains. A more suggestive role of RHB 104 in treating MAP

infection is the synergism between low dosages of the three drugs Clarithromycin, Rifabutin, and Clofazimine in RHB 104. When RHB 104 was compared to each individual drug at low dosages or in dual combinations, we found that RHB 104 is superior in its inhibitory effects against clinical MAP strains. Although RHB 104 is effective against clinical MAP strains *in vitro*, there is still another leading pathogen, AIEC to consider.

The second part of our study was to investigate both MAP and AIEC simultaneously from affected tissues. After countless optimizations and experimentation, we developed a multicolor visualizing method to detect these two pathogens using cultured bacteria. This method using fluorescent *in situ* hybridization was utilized to detect these pathogens from intestinal mucosa of CD patients. We detected both of these pathogens within the lamina propria of the intestinal mucosa with a higher prevalence and greater presence of MAP in CD patients. This may suggest a collusion of both opportunistic pathogens in the pathogenesis of CD as opposed to a solitary agent. However, we should not dismiss the idea of having a primary agent and a secondary agent precipitating the chronic inflammation seen in CD. Further studies need to be done in order to determine the actual role of MAP and AIEC in the pathogenesis of CD.

Although our findings did not establish the causality of MAP and/or AIEC in Crohn's disease, they provided a means of simultaneous investigation of these pathogens *in situ* to advance our understanding of their role in this recurring disease. Our findings also suggested that RHB 104 is a combinatorial antibiotic drug that is efficacious against clinical MAP strains, especially for CD patients with MAP infection.

REFERENCES

1. Stevenson, K., *Genetic diversity of Mycobacterium avium subspecies paratuberculosis and the influence of strain type on infection and pathogenesis: a review.* Vet Res, 2015. **46**: p. 64.
2. Baumgart, D.C. and W.J. Sandborn, *Crohn's disease.* Lancet, 2012. **380**(9853): p. 1590-605.
3. Danese, S., et al., *Development of Red Flags Index for Early Referral of Adults with Symptoms and Signs Suggestive of Crohn's Disease: An IOIBD Initiative.* J Crohns Colitis, 2015. **9**(8): p. 601-6.
4. Selby, W., et al., *Two-year combination antibiotic therapy with clarithromycin, rifabutin, and clofazimine for Crohn's disease.* Gastroenterology, 2007. **132**(7): p. 2313-9.
5. Cury, D.B. and A.C. Moss, *Treatment of Crohn's disease in pregnant women: drug and multidisciplinary approaches.* World J Gastroenterol, 2014. **20**(27): p. 8790-5.
6. Naser, S.A., D. Schwartz, and I. Shafran, *Isolation of Mycobacterium avium subsp paratuberculosis from breast milk of Crohn's disease patients.* Am J Gastroenterol, 2000. **95**(4): p. 1094-5.
7. Chiodini, R.J., et al., *Possible role of mycobacteria in inflammatory bowel disease. I. An unclassified Mycobacterium species isolated from patients with Crohn's disease.* Dig Dis Sci, 1984. **29**(12): p. 1073-9.
8. Mendoza, J.L., et al., *High prevalence of viable Mycobacterium avium subspecies paratuberculosis in Crohn's disease.* World J Gastroenterol, 2010. **16**(36): p. 4558-63.

9. Naser, S.A., et al., *Culture of Mycobacterium avium subspecies paratuberculosis from the blood of patients with Crohn's disease.* Lancet, 2004. **364**(9439): p. 1039-44.

10. Nazareth, N., et al., *Prevalence of Mycobacterium avium subsp. paratuberculosis and Escherichia coli in blood samples from patients with inflammatory bowel disease.* Med Microbiol Immunol, 2015.

11. Chamberlin, W., et al., *Successful treatment of a Crohn's disease patient infected with bacteremic Mycobacterium paratuberculosis.* Am J Gastroenterol, 2007. **102**(3): p. 689-91.

12. Darfeuille-Michaud, A., et al., *Presence of adherent Escherichia coli strains in ileal mucosa of patients with Crohn's disease.* Gastroenterology, 1998. **115**(6): p. 1405-13.

13. Schippa, S., et al., *A potential role of Escherichia coli pathobionts in the pathogenesis of pediatric inflammatory bowel disease.* Can J Microbiol, 2012. **58**(4): p. 426-32.

14. Negroni, A., et al., *Characterization of adherent-invasive Escherichia coli isolated from pediatric patients with inflammatory bowel disease.* Inflamm Bowel Dis, 2012. **18**(5): p. 913-24.

15. Loftus EV, J., Shivashankar R, Tremaine WJ, Harmsen WS, Zinsmeiseter AR. *Updated Incidence and Prevalence of Crohn's Disease and Ulcerative Colitis in Olmsted County, Minnesota (1970-2011).* in *ACG 2014 Annual Scientific Meeting*. October 2014.

16. Burisch, J. and P. Munkholm, *The epidemiology of inflammatory bowel disease.* Scand J Gastroenterol, 2015. **50**(8): p. 942-51.

17. Ooi, C.J., et al., *The Asia Pacific Consensus Statements on Crohn's Disease Part 1: definition, diagnosis and epidemiology.* J Gastroenterol Hepatol, 2015.

18. Esmat, S., et al., *Epidemiological and clinical characteristics of inflammatory bowel diseases in Cairo, Egypt.* World J Gastroenterol, 2014. **20**(3): p. 814-21.

19. Ouakaa-Kchaou, A., et al., *Epidemiological evolution of epidemiology of the inflammatory bowel diseases in a hospital of Tunis.* Tunis Med, 2013. **91**(1): p. 70-3.

20. Alatise, O.I., et al., *Characteristics of inflammatory bowel disease in three tertiary health centers in southern Nigeria.* West Afr J Med, 2012. **31**(1): p. 28-33.

21. Danese, S., et al., *Development of Red Flags Index for Early Referral of Adults with Symptoms and Signs Suggestive of Crohn's Disease: An IOIBD Initiative.* J Crohns Colitis, 2015.

22. Greenstein, R.J. and M.T. Collins, *Emerging pathogens: is Mycobacterium avium subspecies paratuberculosis zoonotic?* Lancet, 2004. **364**(9432): p. 396-7.

23. Borody, T.J., et al., *Anti-mycobacterial therapy in Crohn's disease heals mucosa with longitudinal scars.* Dig Liver Dis, 2007. **39**(5): p. 438-44.

24. Shafran, I., et al., *Open clinical trial of rifabutin and clarithromycin therapy in Crohn's disease.* Dig Liver Dis, 2002. **34**(1): p. 22-8.

25. Rhodes, G., et al., *Mycobacterium avium subspecies paratuberculosis is widely distributed in British soils and waters: implications for animal and human health.* Environ Microbiol, 2013. **15**(10): p. 2761-74.

26. Shankar, H., et al., *Presence, characterization, and genotype profiles of Mycobacterium avium subspecies paratuberculosis from unpasteurized individual and pooled milk, commercial pasteurized milk, and milk products in India by culture, PCR, and PCR-REA methods.* Int J Infect Dis, 2010. **14**(2): p. e121-6.

27. Ricchi, M., et al., *Evaluation of viable Mycobacterium avium subsp. paratuberculosis in milk using peptide-mediated separation and Propidium Monoazide qPCR.* FEMS Microbiol Lett, 2014. **356**(1): p. 127-33.

28. Faria, A.C., et al., *Short communication: Viable Mycobacterium avium subspecies paratuberculosis in retail artisanal Coalho cheese from Northeastern Brazil.* J Dairy Sci, 2014. **97**(7): p. 4111-4.

29. Cirone, K., et al., *Growth of Mycobacterium avium subsp. paratuberculosis, Escherichia coli, and Salmonella Enteritidis during Preparation and Storage of Yogurt.* ISRN Microbiol, 2013. **2013**: p. 247018.

30. Eltholth, M.M., et al., *Contamination of food products with Mycobacterium avium paratuberculosis: a systematic review.* J Appl Microbiol, 2009. **107**(4): p. 1061-71.

31. Grant, I.R., et al., *Inactivation of Mycobacterium paratuberculosis in cows' milk at pasteurization temperatures.* Appl Environ Microbiol, 1996. **62**(2): p. 631-6.

32. Whittington, R.J., et al., *Development and validation of a liquid medium (M7H9C) for routine culture of Mycobacterium avium subsp. paratuberculosis to replace modified Bactec 12B medium.* J Clin Microbiol, 2013. **51**(12): p. 3993-4000.

33. Legrand, E., C. Sola, and N. Rastogi, *[Mycobacterium avium-intracellulare complex: phenotypic and genotypic markers and the molecular basis for interspecies transmission]*. Bull Soc Pathol Exot, 2000. **93**(3): p. 182-92.

34. Romero, C., et al., *Evaluation of surgical tissue from patients with Crohn's disease for the presence of Mycobacterium avium subspecies paratuberculosis DNA by in situ hybridization and nested polymerase chain reaction.* Inflamm Bowel Dis, 2005. **11**(2): p. 116-25.

35. Naser, S., I. Shafran, and F. El-Zaatari, *Mycobacterium avium subsp. paratuberculosis in Crohn's disease is serologically positive.* Clin Diagn Lab Immunol, 1999. **6**(2): p. 282.

36. Tuci, A., et al., *Fecal detection of Mycobacterium avium paratuberculosis using the IS900 DNA sequence in Crohn's disease and ulcerative colitis patients and healthy subjects.* Dig Dis Sci, 2011. **56**(10): p. 2957-62.

37. Singh, A.V., et al., *Presence and characterization of Mycobacterium avium subspecies paratuberculosis from clinical and suspected cases of Crohn's disease and in the healthy human population in India.* Int J Infect Dis, 2008. **12**(2): p. 190-7.

38. Gasparetto, M., I. Angriman, and G. Guariso, *The multidisciplinary health care team in the management of stenosis in Crohn's disease.* J Multidiscip Healthc, 2015. **8**: p. 167-79.

39. Funayama, Y., et al., *[Surgical management of intestinal Crohn's disease]*. Nihon Geka Gakkai Zasshi, 2015. **116**(2): p. 94-8.

40. Bharadwaj, S., P. Fleshner, and B. Shen, *Therapeutic Armamentarium for Stricturing Crohn's Disease: Medical Versus Endoscopic Versus Surgical Approaches.* Inflamm Bowel Dis, 2015.

41. Chang, C.W., et al., *Intestinal stricture in Crohn's disease.* Intest Res, 2015. **13**(1): p. 19-26.

42. Cayci, M., et al., *The analysis of clinico-pathologic characteristics in patients who underwent surgery due to stricturing and non-perineal fistulizing forms of Crohn's disease: a retrospective cohort study.* Int J Surg, 2015. **15**: p. 49-54.

43. Mosli, M.H. and B.G. Feagan, *Combination therapy for the treatment of Crohn's disease.* Expert Opin Biol Ther, 2015: p. 1-14.

44. Donnellan, C.F., L.H. Yann, and S. Lal, *Nutritional management of Crohn's disease.* Therap Adv Gastroenterol, 2013. **6**(3): p. 231-42.

45. Lahad, A. and B. Weiss, *Current therapy of pediatric Crohn's disease.* World J Gastrointest Pathophysiol, 2015. **6**(2): p. 33-42.

46. Nuti, F., G. Fiorino, and S. Danese, *Adalimumab for the treatment of pediatric Crohn's disease.* Expert Rev Clin Immunol, 2015: p. 1-10.

47. Prescott, S.M., et al., *Platelet-activating factor and related lipid mediators.* Annu Rev Biochem, 2000. **69**: p. 419-45.

48. Punchard, N.A., S.M. Greenfield, and R.P. Thompson, *Mechanism of action of 5-arninosalicylic acid.* Mediators Inflamm, 1992. **1**(3): p. 151-65.

49. Gisbert, J.P., et al., *Role of 5-aminosalicylic acid (5-ASA) in treatment of inflammatory bowel disease: a systematic review.* Dig Dis Sci, 2002. **47**(3): p. 471-88.

50. Chang, M.I., B.L. Cohen, and A.J. Greenstein, *A review of the impact of biologics on surgical complications in Crohn's disease.* Inflamm Bowel Dis, 2015. **21**(6): p. 1472-7.

51. Nuti, F., et al., *Prospective Evaluation Of The Achievement Of Mucosal Healing With Anti-With TNF-alpha Therapy In A Pediatric Crohn'S Disease Cohort.* J Crohns Colitis, 2015.

52. O'Toole, A. and A.C. Moss, *Optimizing Biologic Agents in Ulcerative Colitis and Crohn's Disease.* Curr Gastroenterol Rep, 2015. **17**(8): p. 453.

53. Meyer, L., et al., *[Adverse events associated with the treatment of inflammatory bowel disease]*. Rev Med Chil, 2015. **143**(1): p. 7-13.

54. Luo, Y., et al., *Short-Term Efficacy of Exclusive Enteral Nutrition in Pediatric Crohn's Disease: Practice in China.* Gastroenterol Res Pract, 2015. **2015**: p. 428354.

55. Whitman, M.S. and A.R. Tunkel, *Azithromycin and clarithromycin: overview and comparison with erythromycin.* Infect Control Hosp Epidemiol, 1992. **13**(6): p. 357-68.

56. Hewitt, R.G., et al., *Prevention of disseminated Mycobacterium avium complex infection with reduced dose clarithromycin in patients with advanced HIV disease.* AIDS, 1999. **13**(11): p. 1367-72.

57. Dunne, M., et al., *A randomized, double-blind trial comparing azithromycin and clarithromycin in the treatment of disseminated Mycobacterium avium infection in patients with human immunodeficiency virus.* Clin Infect Dis, 2000. **31**(5): p. 1245-52.

58. Maddix, D.S., K.B. Tallian, and P.S. Mead, *Rifabutin: a review with emphasis on its role in the prevention of disseminated Mycobacterium avium complex infection.* Ann Pharmacother, 1994. **28**(11): p. 1250-4.

59. Shafran, S.D., et al., *Does in vitro susceptibility to rifabutin and ethambutol predict the response to treatment of Mycobacterium avium complex bacteremia with rifabutin, ethambutol, and clarithromycin? Canadian HIV Trials Network Protocol 010 Study Group.* Clin Infect Dis, 1998. **27**(6): p. 1401-5.

60. Pinheiro, M., et al., *The influence of rifabutin on human and bacterial membrane models: implications for its mechanism of action.* J Phys Chem B, 2013. **117**(20): p. 6187-93.

61. Clancy, C.J., et al., *Inhibition of RNA synthesis as a therapeutic strategy against Aspergillus and Fusarium: demonstration of in vitro synergy between rifabutin and amphotericin B.* Antimicrob Agents Chemother, 1998. **42**(3): p. 509-13.

62. Shafran, S.D., et al., *A comparison of two regimens for the treatment of Mycobacterium avium complex bacteremia in AIDS: rifabutin, ethambutol, and clarithromycin versus*

rifampin, ethambutol, clofazimine, and ciprofloxacin. Canadian HIV Trials Network Protocol 010 Study Group. N Engl J Med, 1996. **335**(6): p. 377-83.

63. Borody, T.J., et al., *Treatment of severe Crohn's disease using antimycobacterial triple therapy--approaching a cure?* Dig Liver Dis, 2002. **34**(1): p. 29-38.

64. Gui, G.P., et al., *Two-year-outcomes analysis of Crohn's disease treated with rifabutin and macrolide antibiotics.* J Antimicrob Chemother, 1997. **39**(3): p. 393-400.

65. Yano, T., et al., *Reduction of clofazimine by mycobacterial type 2 NADH:quinone oxidoreductase: a pathway for the generation of bactericidal levels of reactive oxygen species.* J Biol Chem, 2011. **286**(12): p. 10276-87.

66. Zhang, S., et al., *Identification of novel mutations associated with clofazimine resistance in Mycobacterium tuberculosis.* J Antimicrob Chemother, 2015.

67. Krishnan, M.Y., E.J. Manning, and M.T. Collins, *Effects of interactions of antibacterial drugs with each other and with 6-mercaptopurine on in vitro growth of Mycobacterium avium subspecies paratuberculosis.* J Antimicrob Chemother, 2009. **64**(5): p. 1018-23.

68. Hafner, R., et al., *Tolerance and pharmacokinetic interactions of rifabutin and clarithromycin in human immunodeficiency virus-infected volunteers.* Antimicrob Agents Chemother, 1998. **42**(3): p. 631-9.

69. Rastogi, N., K.S. Goh, and V. Labrousse, *Activity of clarithromycin compared with those of other drugs against Mycobacterium paratuberculosis and further enhancement of its extracellular and intracellular activities by ethambutol.* Antimicrob Agents Chemother, 1992. **36**(12): p. 2843-6.

70. Chiodini, R.J., *Bactericidal activities of various antimicrobial agents against human and animal isolates of Mycobacterium paratuberculosis.* Antimicrob Agents Chemother, 1990. **34**(2): p. 366-7.

71. Zanetti, S., et al., *"In vitro" activities of antimycobacterial agents against Mycobacterium avium subsp. paratuberculosis linked to Crohn's disease and paratuberculosis.* Ann Clin Microbiol Antimicrob, 2006. **5**: p. 27.

72. Pierce, E.S., *Where are all the Mycobacterium avium subspecies paratuberculosis in patients with Crohn's disease?* PLoS Pathog, 2009. **5**(3): p. e1000234.

73. Dalziel, T.K., *Thomas Kennedy Dalziel 1861-1924. Chronic interstitial enteritis.* Dis Colon Rectum, 1989. **32**(12): p. 1076-8.

74. Burnham, W.R., et al., *Mycobacteria as a possible cause of inflammatory bowel disease.* Lancet, 1978. **2**(8092 Pt 1): p. 693-6.

75. Sanderson, J.D., et al., *Mycobacterium paratuberculosis DNA in Crohn's disease tissue.* Gut, 1992. **33**(7): p. 890-6.

76. Moss, M.T., et al., *Polymerase chain reaction detection of Mycobacterium paratuberculosis and Mycobacterium avium subsp silvaticum in long term cultures from Crohn's disease and control tissues.* Gut, 1992. **33**(9): p. 1209-13.

77. Schwartz, D., et al., *Use of short-term culture for identification of Mycobacterium avium subsp. paratuberculosis in tissue from Crohn's disease patients.* Clin Microbiol Infect, 2000. **6**(6): p. 303-7.

78. Lisby, G., et al., *Mycobacterium paratuberculosis in intestinal tissue from patients with Crohn's disease demonstrated by a nested primer polymerase chain reaction.* Scand J Gastroenterol, 1994. **29**(10): p. 923-9.

79. Gan, H., Q. Ouyang, and H. Bu, *[Mycobacterium paratuberculosis in the intestine of patients with Crohn's disease]*. Zhonghua Nei Ke Za Zhi, 1997. **36**(4): p. 228-30.

80. Fidler, H.M., et al., *Specific detection of Mycobacterium paratuberculosis DNA associated with granulomatous tissue in Crohn's disease.* Gut, 1994. **35**(4): p. 506-10.

81. Dell'Isola, B., et al., *Detection of Mycobacterium paratuberculosis by polymerase chain reaction in children with Crohn's disease.* J Infect Dis, 1994. **169**(2): p. 449-51.

82. Sechi, L.A., et al., *Identification of Mycobacterium avium subsp. paratuberculosis in biopsy specimens from patients with Crohn's disease identified by in situ hybridization.* J Clin Microbiol, 2001. **39**(12): p. 4514-7.

83. Naser, S.A., et al., *In situ identification of mycobacteria in Crohn's disease patient tissue using confocal scanning laser microscopy.* Mol Cell Probes, 2002. **16**(1): p. 41-8.

84. Keown, D.A., D.A. Collings, and J.I. Keenan, *Uptake and persistence of Mycobacterium avium subsp. paratuberculosis in human monocytes.* Infect Immun, 2012. **80**(11): p. 3768-75.

85. Warth, A., *Is alpha-dystroglycan the missing link in the mechanism of enterocyte uptake and translocation of Mycobacterium avium paratuberculosis?* Med Hypotheses, 2008. **70**(2): p. 369-74.

86. Cheville, N.F., et al., *Intracellular trafficking of Mycobacterium avium ss. paratuberculosis in macrophages.* Dtsch Tierarztl Wochenschr, 2001. **108**(6): p. 236-43.

87. Rumsey, J., J.F. Valentine, and S.A. Naser, *Inhibition of phagosome maturation and survival of Mycobacterium avium subspecies paratuberculosis in polymorphonuclear leukocytes from Crohn's disease patients.* Med Sci Monit, 2006. **12**(4): p. BR130-9.

88. Mann, E.R. and X. Li, *Intestinal antigen-presenting cells in mucosal immune homeostasis: crosstalk between dendritic cells, macrophages and B-cells.* World J Gastroenterol, 2014. **20**(29): p. 9653-64.

89. Glasser, A.L., et al., *Adherent invasive Escherichia coli strains from patients with Crohn's disease survive and replicate within macrophages without inducing host cell death.* Infect Immun, 2001. **69**(9): p. 5529-37.

90. Boudeau, J., N. Barnich, and A. Darfeuille-Michaud, *Type 1 pili-mediated adherence of Escherichia coli strain LF82 isolated from Crohn's disease is involved in bacterial invasion of intestinal epithelial cells.* Mol Microbiol, 2001. **39**(5): p. 1272-84.

91. Boudeau, J., et al., *Invasive ability of an Escherichia coli strain isolated from the ileal mucosa of a patient with Crohn's disease.* Infect Immun, 1999. **67**(9): p. 4499-509.

92. Darfeuille-Michaud, A., et al., *High prevalence of adherent-invasive Escherichia coli associated with ileal mucosa in Crohn's disease.* Gastroenterology, 2004. **127**(2): p. 412-21.

93. Conte, M.P., et al., *Adherent-invasive Escherichia coli (AIEC) in pediatric Crohn's disease patients: phenotypic and genetic pathogenic features.* BMC Res Notes, 2014. **7**: p. 748.

94. Fujita, H., et al., *Quantitative analysis of bacterial DNA from Mycobacteria spp., Bacteroides vulgatus, and Escherichia coli in tissue samples from patients with inflammatory bowel diseases.* J Gastroenterol, 2002. **37**(7): p. 509-16.

95. Gordon, D.M., et al., *Assigning Escherichia coli strains to phylogenetic groups: multi-locus sequence typing versus the PCR triplex method.* Environ Microbiol, 2008. **10**(10): p. 2484-96.

96. Desilets, M., et al., *Genome-based Definition of an Inflammatory Bowel Disease-associated Adherent-Invasive Escherichia coli Pathovar.* Inflamm Bowel Dis, 2015.

97. Gall, J.G. and M.L. Pardue, *Formation and detection of RNA-DNA hybrid molecules in cytological preparations.* Proc Natl Acad Sci U S A, 1969. **63**(2): p. 378-83.

98. Pardue, M.L. and J.G. Gall, *Molecular hybridization of radioactive DNA to the DNA of cytological preparations.* Proc Natl Acad Sci U S A, 1969. **64**(2): p. 600-4.

99. Rudkin, G.T. and B.D. Stollar, *High resolution detection of DNA-RNA hybrids in situ by indirect immunofluorescence.* Nature, 1977. **265**(5593): p. 472-3.

100. Klaassens, M., et al., *Congenital diaphragmatic hernia and chromosome 15q26: determination of a candidate region by use of fluorescent in situ hybridization and array-based comparative genomic hybridization.* Am J Hum Genet, 2005. **76**(5): p. 877-82.

101. Arnoldi, J., et al., *Species-specific assessment of Mycobacterium leprae in skin biopsies by in situ hybridization and polymerase chain reaction.* Lab Invest, 1992. **66**(5): p. 618-23.

102. Amann, R. and B.M. Fuchs, *Single-cell identification in microbial communities by improved fluorescence in situ hybridization techniques.* Nat Rev Microbiol, 2008. **6**(5): p. 339-48.

103. Baumgart, M., et al., *Culture independent analysis of ileal mucosa reveals a selective increase in invasive Escherichia coli of novel phylogeny relative to depletion of Clostridiales in Crohn's disease involving the ileum.* ISME J, 2007. **1**(5): p. 403-18.

104. Le Puil, M., et al., *A novel fluorescence imaging technique combining deconvolution microscopy and spectral analysis for quantitative detection of opportunistic pathogens.* J Microbiol Methods, 2006. **67**(3): p. 597-602.

105. Simpson, K.W., et al., *Adherent and invasive Escherichia coli is associated with granulomatous colitis in boxer dogs.* Infect Immun, 2006. **74**(8): p. 4778-92.

106. Sasikala, M., et al., *Absence of Mycobacterium avium ss paratuberculosis-specific IS900 sequence in intestinal biopsy tissues of Indian patients with Crohn's disease.* Indian J Gastroenterol, 2009. **28**(5): p. 169-74.

107. Parrish, N.M., et al., *Absence of mycobacterium avium subsp. paratuberculosis in Crohn's patients.* Inflamm Bowel Dis, 2009. **15**(4): p. 558-65.

108. Lozano-Leon, A., M. Barreiro-de Acosta, and J.E. Dominguez-Munoz, *Absence of Mycobacterium avium subspecies paratuberculosis in Crohn's disease patients.* Inflamm Bowel Dis, 2006. **12**(12): p. 1190-2.

109. Ellingson, J.L., et al., *Absence of Mycobacterium avium subspecies paratuberculosis components from Crohn's disease intestinal biopsy tissues.* Clin Med Res, 2003. **1**(3): p. 217-26.

110. Baksh, F.K., et al., *Absence of Mycobacterium avium subsp. paratuberculosis in the microdissected granulomas of Crohn's disease.* Mod Pathol, 2004. **17**(10): p. 1289-94.